Neurochemistry International 147 (2021) 105064

Contents lists available at ScienceDirect

Neurochemistry International

journal homepage: www.elsevier.com/locate/neuint

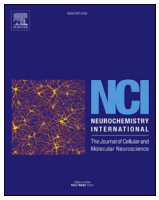

Multitarget neuroprotection by quercetin: Changes in gene expression in two perinatal asphyxia models

V. Cardozo [a,1], L. Vaamonde [b,1], A. Parodi-Talice [a,c,1], M.J. Zuluaga [d], D. Agrati [d], M. Portela [e,f], A. Lima [e,h], F. Blasina [b,**], F. Dajas [g], G. Bedó [a,*]

[a] Sección Genética Evolutiva, Facultad de Ciencias, Universidad de la República (Udelar), Montevideo, Uruguay
[b] Dept. Neonatología, Facultad de Medicina, Universidad de la República (Udelar), Montevideo, Uruguay
[c] Unidad de Biología Molecular, Institut Pasteur de Montevideo, Montevideo, Uruguay
[d] Sección Fisiología y Nutrición, Facultad de Ciencias, Universidad de la República (Udelar), Montevideo, Uruguay
[e] Unidad de Bioquímica y Proteómica Analíticas, Institut Pasteur de Montevideo
[f] Facultad de Ciencias, Universidad de la República (Udelar), Montevideo, Uruguay
[g] Dept. Neuroquímica, Instituto de Investigaciones Biológicas Clemente Estable, Ministerio de Educación y Cultura, Montevideo, Uruguay
[h] Instituto de Investigaciones Biológicas Clemente Estable, Ministerio de Educación y Cultura, Montevideo, Uruguay

ARTICLE INFO

Keywords:
Perinatal asphyxia
Neuroprotection
Quercetin
Proteomics

ABSTRACT

Hypoxic-ischemic encephalopathy (HIE) causes mortality and long-term neurologic morbidities in newborns, affecting pathways related to energy failure, excitotoxicity and oxidative stress that often lead to cell death. The whole process of HIE injury is coupled to changes in the expression of a great array of proteins. A nanoliposomal preparation of the flavonoid quercetin has been shown to exert neuroprotective effects in perinatal asphyxia models.

This study aimed to identify neonatal HIE markers and explore the effect of quercetin administration in two perinatal asphyxia models: newborn rats and piglets. In the rat model, nanoliposomal quercetin administration reduced mortality after asphyxia. In the piglet model, quercetin partially overrode the reduction of HIF-1α mRNA levels in the cortex induced by asphyxia. Quercetin administration also reduced increased level of HO-1 mRNA in asphyctic piglets. These results suggest that quercetin neuroprotection might be involved in the regulation of HIF-1α, HO-1 and their targets.

A proteomic approach revealed that the glycolytic pathway is strongly regulated by quercetin in both species. We also identified a set of proteins differentially expressed that could be further considered as markers. In piglets, this set includes Acidic Leucine-rich nuclear phosphoprotein 32 (ANP32A), associated with nervous system differentiation, proteins related with death pathways and alpha-enolase which can be converted to neuron-specific enolase, a glycolytic enzyme that may promote neuroprotection. In newborn rats, other promising proteins associated with neurogenesis and neuroprotection emerged, such as dihydropyrimidinase-related proteins, catalytic and regulatory subunits of phosphatases and heterogeneous nuclear ribonucleoprotein K (hnRNPK).

Our results show that a nanoliposomal preparation of quercetin, with protective effect in two HIE mammal models, modulates the expression of proteins involved in energy metabolism and other putative neuroprotective signals in the cortex. Identification of these signals could reveal potential molecular pathways involved in disease onset and the novel quercetin neuroprotective strategy.

* Corresponding author. Sección Genética Evolutiva, Facultad de Ciencias, Universidad de la República (Udelar), Montevideo, Uruguay.
** Corresponding author. Dept. Neonatología, Facultad de Medicina, Univerdidad de la República (Udelar), Montevideo, Uruguay.
E-mail addresses: fblasina@hc.edu.uy (F. Blasina), gbedo@fcien.edu.uy, bedogabriela@gmail.com (G. Bedó).
[1] These authors contribute equally to this work and should be considered as co-first authors.

https://doi.org/10.1016/j.neuint.2021.105064
Received 27 August 2020; Received in revised form 26 April 2021; Accepted 27 April 2021
Available online 2 May 2021

1. Introduction

Hypoxic-ischemic encephalopathy (HIE) secondary to perinatal asphyxia (PA) is one of the main causes of mortality in newborns and has been associated with long-term neurologic morbidities in the surviving neonate (Kurinczuk et al., 2010; Liu et al., 2016). Despite progress in neonatal care in the past decades, neonatal HIE still has a prevalence of 1–6 per 1000 live births. About 15%–20% of affected newborns die in the postnatal period, and around 30%–70% suffer neurological disabilities that, depending on the severity of the HIE (Shankaran, 2012), lead to different pathological entities such as cerebral palsy and mental retardation, epilepsy, attention deficit, hyperactivity and other late-onset neuropsychiatric syndromes (Du Plessis and Volpe, 2002; Fleiss and Gressens, 2019; Odd et al., 2009; Van Erp et al., 2002).

The search for neuroprotective strategies is hindered by the complexity of the HIE injury (Rodríguez et al., 2020). In this regard, deepening the comprehension of still unknown molecular aspects of HIE and the putative effect of new treatments could help to identify biomarkers and to develop an effective combination of treatments.

In the initial phase of the HIE insult, glucose and oxygen deprivation leads to an energy failure followed by glutamate-mediated excitotoxicity and Na+/K + ATPase failure resulting in cell death. The increase in intracellular calcium is followed by an excitotoxic cycle (Pierson et al., 2007). Further consequences include the formation of free radicals, production of nitric oxide and lipid peroxidation of cell membranes. Neuronal necrosis is the most common and severe type of brain injury during the primary hypoxic-ischemic insult (Rainaldi and Perlman, 2016). During reperfusion, a secondary energy failure phase occurs (delayed phase), starting approximately 6 h or up to 24 h after the initial injury and characterized by mitochondrial dysfunction and initiation of the apoptotic cascade. This injury is characterized by inflammation, generation of reactive oxygen species and free radicals and cell death, induced mainly through caspase-3 activation (Vannucci and Hagberg, 2004). The tertiary phase is characterized by remodeling and tissue recovery involving new cell development and recovery of surviving neuronal circuits.

The initial biphasic pattern of brain neonatal injury allows for a "therapeutic window" of 6 h from birth, essential for the application of neuroprotective strategies, such as hypothermia (Davidson et al., 2015). Although the neurotoxic cascade is already activated and mitochondrial impairment may exist during this latent phase, neuroprotective therapies can be applied and would benefit from markers revealing hypoxia severity and recovery (Iwata et al., 2008; van Bel and Groenendaal, 2016; Rodríguez et al., 2020).

Cellular response to hypoxia implies coordinated regulation of the expression of a large number of genes. The changes in gene expression are initially targeted to minimize damage and save energy to provide compensation for hypoxia (Dai et al., 2014; Hochachka and Lutz, 2001). A second response depending on gene expression modulation can lead to cell death if the damage is irreversible or activate cell survival-promoting programs. It has been reported that Hypoxia-inducible factor-1 α (HIF-1α) expression constitutes an early immediate response to oxygen deprivation and triggers the regulation of several downstream molecules (Chiral et al., 2004) which play a fundamental role in ensuring tight regulation of oxygen homeostasis in the brain.

The selection of the most suitable treatment as well as the optimal timing for applying it is a challenge for scientists and neonatologists. So far, the only standardized treatment for moderate to severe HIE is therapeutic hypothermia initiated within 6 h from birth. However, this strategy is only partially effective (Merchant and Azzopardi, 2015) and is not used in all gestational ages since it is not applicable during the whole preterm period (Laptook, 2016). It is possible that a combination of several therapeutic strategies will be necessary to block cell death and improve functional outcome (Onténiente et al., 2003). Thus, the use of adjunct therapies has become an increasing focus of study and other combined treatments are currently being assayed (Rao et al., 2017; Glass, 2018; Osier et al., 2018). Effective neuroprotective strategies will need to target multiple pathways and reflect the regional and temporal changes underlying the diverse neuronal cell death phenotypes. As hypothermia for neonatal HIE impacts different cytoplasmic pathways -such as the oxidative cascade, mitochondrial failure, free radicals, lipid peroxidation and inflammation-it might be beneficial to use it in combination with other multitarget neuroprotective compounds.

In the last few years, several studies have pointed to the role of natural antioxidants as neuroprotective agents in neurodegenerative and vascular disorders (Rendeiro et al., 2009; Rivera et al., 2008; Silva et al., 2008). Flavonoids have been identified as potent agents with a protective profile (Dajas et al., 2003; Mandel et al., 2012; Patil et al., 2003). Quercetin, a flavonoid ubiquitous in plants, fruits, and vegetables, protects neurons in culture against oxidative stress insults and neurons in *in vivo* models against focal ischemia or trauma (Dajas, 2012; Dajas et al., 2015; Ossola et al., 2009) in different mammal newborn models of HIE (Qu et al., 2014; Blasina et al., 2015; Le et al., 2020). The beneficial effects of quercetin as an antioxidant, anti-inflammatory and promoter of gene expression of survival proteins make it a potential therapeutic tool for HIE. Blasina et al. (2015) developed a nanoliposomal preparation of quercetin and demonstrated its effects in a perinatal asphyxia model in newborn piglets, showing it could be an appropriate strategy to combine with therapeutic hypothermia. This nanoliposomal preparation improved brain bioavailability of quercetin as a concentration of 10 mg/kg administered intravenously stabilized blood pressure after a severe hypoxic episode and promoted recovery of brain function as shown in EEG amplitude recordings obtained either 8 or 72 h after the asphyctic episode (Blasina et al., 2015).

Even though nanoliposome deposition in the brain can be achieved through different routes of administration (oral, transdermal, intravenous, intramuscular, intraperitoneal, etc.) (Danaei et al., 2018), the intranasal route is less invasive. The surface area of the nasal mucosa ensures rapid absorption of most drugs and avoids the first-pass metabolism associated with oral administration, thus bypassing the gastrointestinal system (Marx et al., 2015). Despite its advantages, intranasal administration is not frequently used or tested, and has hardly ever been assayed for quercetin administration. The neuroprotective effects of intranasal breast milk in human preterms with intracerebral severe hemorrhage was explored in a recent study, proving intranasal administration as a useful and promising drug delivery strategy (Keller et al., 2019). Based on this evidence, we decided to test the potential of the nanoliposomal preparation along with intranasal administration in the newborn rat.

Numerous models of hypoxia and hypoxia-ischemia (HI) have been developed in rodents and in larger species to mimic the different types of injuries seen in the human newborn (Mallard and Vexler, 2015). In the present work, we took advantage of experimental procedures in two different species extensively used to explore perinatal asphyxia pathophysiology: newborn piglets with perinatal asphyxia as a livestock model (Blasina et al., 2015; Roth and Tuggle, 2015) and the rat model of immersion asphyxia described as "delayed cesarean section" (Bjelke et al., 1991). Newborn piglets subjected to different combinations of hypoxia and ischemia show changes in metabolism (magnetic resonance spectroscopy), cerebral blood flow (CBF) and electric response like those observed in human infants with HIE. In general, injury in this species is characterized by neuronal loss in the sensorimotor cortex and basal ganglia and by postnatal seizures. The piglet model has been critical in the development of therapeutic hypothermia for newborns with HIE (Thoresen et al., 1995) and particularly useful in translational research considering that in newborn piglets brain and organ maturation at-term is similar to that of humans, they have gyrencephalic brains and a white/gray matter ratio similar to the human brain (Roth and Tuggle 2015).

Rodents, in turn, are not a gyrencephalic species and their physiology, CBF regulation and white/gray matter ratios are vastly different

from those of humans. Nevertheless, many HIE models have been developed in rodents due to ease of maintenance, short life cycle and abundant genetic resources. Inducing asphyxia at delivery in this model has several advantages: (i) it mimics well some relevant aspects of human delivery; (ii) it is a low-invasive procedure; (iii) it allows studying short- and long-term consequences of the insult in the same preparation, and (iv) it is highly reproducible (Herrera-Marschitz et al., 2011). Given their differences, the complementary contributions of the two models allow for a better understanding of the events following short and severe asphyxia.

This study aimed to deepen the knowledge of the processes occurring during and after perinatal asphyxia injury in these two neonatal models and to characterize the effect of quercetin administration, analyzing the pathways implied in this protection and identifying potential markers. Of particular interest is the analysis at protein level because changes that occur during hypoxia-reoxygenation and/or after neuroprotective treatment occur mainly at a post-transcriptional level.

2. Material and methods

2.1. Animals and experimental neonatal HI injury models

In the two models we applied different experimental procedures of perinatal asphyxia and reoxygenation to cause a neonatal hypoxic-ischemic injury (HIE). For this reason, experimental groups subjected to these procedures will be hereafter referred to as “Hypoxia (H)”.

2.1.1. Newborn piglets (Sus scrofa domestica) and normocapnic alveolar induced hypoxia

2.1.1.1. Animals. Animal care and experimental procedures were performed in accordance with the U.K. Animals (Scientific Procedures) Act, 1986 and associated guidelines, EU Directive 2010/63/EU for animal experiments, and the National Institutes of Health guide for the care and use of Laboratory animals (NIH Publications No. 8023, revised 1978). The National Committee on Animal Experimentation approved the experiment protocol (file number 071140-000261-11, CHEA, School of Medicine, approved June 1, 2011). Male newborn piglets (*Sus scrofa domestica*) up to 48 h old with a body weight of 1500 g–2000 g were transported from a local farm (Pando, Canelones, Uruguay) to the University Hospital on the day of the experiment. The preference for male piglets was based on the high susceptibility of males to HI and to eliminate possible differences related to endocrinological responses.

2.1.1.2. Surgical procedure. Anesthetic induction was performed with Ketamine 30 mg/kg i/m, and a mixture of Ketamine 3 mg/kg/h, Midazolam 0.3 mg/kg/h and Fentanyl 10 μg/kg/h i/v was added for anesthetic maintenance. During the experiment, the animals were administered intravenous 5% glucose serum at a rate of 70 ml/kg/day to account for the basal intake of fluids and glucose. Airway access was secured via tracheostomy, initiating ventilation with a mechanical ventilator (Neumovent®, GraphNet). The initial ventilatory parameters were: respiratory rate (RR) of 20 breaths per minute (BPM), positive end-expiratory pressure (PEEP) of 4 cm H_2O, positive inspiratory pressure (MIP) to obtain an exhaled tidal volume of 4–6 ml/kg, inspiratory time consistent with the time constant (according to the flow-time curve) and an inspired fraction of oxygen (FiO_2) required for 90–95% saturation. The expected basal blood gases were pH 7.25–7.35 $PaCO_2$ 35–45 mmHg, PaO_2 50–80 mmHg, Lactic <3 mmol/l. A femoral artery route (continuous invasive monitoring of arterial pressure and extraction of blood samples) and a femoral venous route (perfusion of basal hydration and drugs) were inserted at the beginning of the experiment. A single dose of Cefradine 50 mg/kg/dose i/v and Gentamicin 4.5 mg/kg/dose i/v was administered for prophylactic purposes. Temperature was maintained between 38.5 and 39.5 °C using a thermal crib and a heater (ThermaCare Heater, Gaymar Industries, Inc., NY 14127, USA), and animals were covered with a plastic blanket. Pulse oximetry and esophageal core temperature were continuously monitored (enGuard CM4 monitor, Masimo SET, Ohmeda Medical). Additionally, a one-channel electroencephalogram (EEG) on the left and right parietal position was recorded (inter-electrode distance of 3 cm) for amplitude-integrated encephalography (Olympic Cerebral Function Monitor (CFM), Brainz, Natus®) before, during, and for 8 h after the experimental severe hypoxia. Skin impedance was lowered by shaving and washing of the head, and impedance of the surface electrodes was always <10 k Ω during the recordings.

2.1.1.3. Hypoxia induction. After a 30–60 min stabilization period, defined as a <10% variation in hemodynamic parameters and normal blood gases, the experimental hypoxemia protocol was performed as previously described by Blasina et al. (2015), inducing normocapnic alveolar hypoxia. Each piglet was ventilated with FiO_2 0.08 by increasing the inhaled concentration of nitrogen gas during an individually variable period, which led to severe hypoxemia evidenced by a CFM below 7 μV for at least 17 min and metabolic acidosis. Hypoxia was followed by reoxygenation with FiO_2 1.0 for 30 min (to induce more severe damage) and then 0.21 for the remaining experimental period of 8 h after the beginning of hypoxia.

2.1.1.4. Experimental procedure. Piglets were administered nanoliposomal quercetin formulation intravenously (10 mg/kg) during the reanimation period up to 60 min after hypoxia. If severe hypotension occurred during the reoxygenation period, adrenaline (1 mg/kg/dose) was administered. Animals were divided into the following groups: 1) sham-lesioned (S), 2) hypoxia plus vehicle (nanoliposomal preparation without quercetin) (HV), and 3) hypoxia plus 10 mg/kg nanoliposomal quercetin preparation (HQ). From each group n = 4 were subjected to proteomic analyses and n = 6 to real-time PCR.

At the end of the 8-h experiment, piglets of all three experimental groups under deep anesthesia were euthanized with potassium chloride (20 mEq/l) and their brains were dissected and frozen in liquid nitrogen. Samples were immediately stored at −80 °C for further evaluation of HIF-1α and HO-1 expression at mRNA level or changes induced by hypoxia and administration of quercetin using a 2D electrophoresis proteomic approach.

2.1.2. Rat (Rattus norvegicus) and immersion model of asphyxia

2.1.2.1. Animals. Animal care and experimental procedures were performed in accordance with the Guide for the Care and Use of Laboratory Animals of the NIH and the Uruguayan law (Law 18 611) on animal experimentation. The experimental protocol was approved by the Ethical Committee on Animal Care and Protocols of the Facultad de Ciencias, Universidad de la República (Protocol number 240011-002308-14).

In the present study 0–1 day old male and female newborn rats (*Rattus norvegicus*, Wistar strain) were used. Pups were obtained from pregnant rats housed in separate cages at gestation day 14 and kept in a controlled temperature (22 + 1 °C) and humidity (65%) room under a 12-hr light-dark cycle (lights on at 0600 h), with free access to food and water. On gestational day 21, female rats were periodically checked for their delivery of pups. A group was used as surrogate mothers and the rest were subjected to perinatal asphyxia to obtain the experimental groups.

2.1.2.2. Perinatal asphyxia procedure. The asphyxia was produced by a ‘delayed cesarean section’ as described in Bjelke et al. (1991), with minor modifications. After the first pup was delivered vaginally, full-term pregnant rats were rapidly decapitated, and immediately hysterectomized. Both uterine horns, containing the fetuses, were

immersed in a 37 °C bath for 15 min. Following asphyxia, the uterus horns were rapidly opened, pups were removed and breathing was stimulated by cleaning the amniotic fluid and gentle tapping with small medical wipes for a few minutes until regular breathing became regular. The umbilical cord was ligated and the animals were left to recover on a heating mat.

2.1.2.3. Experimental procedure. Nanoliposomal quercetin (2 mg/ml) was prepared up to 48 h before the trial. In all cases a dose of 10 mg/kg was administered after asphyxia or after control cesarean section, in a single intraperitoneal dose. The sham group was administered the same volume of vehicle (empty nanoliposomes without quercetin). Thus, pups were divided into the following groups: sham plus vehicle (SV); sham plus quercetin (SQ); cesarean section followed by asphyxia to induce hypoxia plus vehicle (HV) or plus quercetin administration (HQ). When their physiological conditions improved, they were given to surrogate mothers who had delivered normally within the 24 h prior to the experiments. Each surrogate mother took care of a litter of eight sham or perinatal asphyxia pups.

This model was applied in this study for quercetin bioavailability and protection assessment: the number of surviving pups in each group was recorded 24 h after reanimation. For the DIGE proteomic approach, the animals were subjected to the asphyxia protocol, and 5 h after reanimation and treatment, a female pup from each experimental group was euthanized. Samples of different brain regions were dissected and immediately stored at −80 °C.

As a complementary study, 24-h old naturally delivered pups were administered intranasal quercetin for the double purpose of assessing its bioavailability and evaluating an easy drug delivery strategy.

2.2. Nanoliposomal formulation

Lecithin/cholesterol/2HBCD lipo-nanosomes of quercetin were obtained in volumes of 20 ml in a reactor device where the mixture reacted under specified conditions of flow, pressure, and temperature (60 °C) in a physiological solution after initial sonication of the lecithin/cholesterol mixture for 24 h (patent application number PCT/IB 2013/059067).

2.3. Bioavailability and quercetin administration in rats

Quercetin concentration in the brain was determined 30 min after either intranasal (n = 4) or intraperitoneal (n = 5) administration to control pups 24 h after delivery. Intraperitoneal administration consisted of a single dose while intranasal quercetin was administered in small volumes over a 60-min period on account of the small size of pups' nostrils. Volumes of 2 μl were administered using Hamilton syringe with cannula (PE 10, 0.28 mm inside diameter) every 4 min, alternating nostrils.

At the specified time point, the offspring were sacrificed and their brains dissected, washed in saline solution and immediately frozen at −80 °C. These samples were analyzed by HPLC with electrochemical detection in the Department of Neurochemistry of the Instituto de Investigaciones Biológicas Clemente Estable, following a standard protocol with modifications (Azuma et al., 2002), as previously published (Martínez-Busi et al., 2019). Briefly, methanol 90% (solvent A)/formic acid 0.1% pH = 2 (solvent B) was used as a mobile phase. The gradient elution program was performed as follows: 0–30 min, 35%–55% A; 30–55 min. 55% A, back to the initial conditions for another 15 min, and the detection wavelength was set at 375 nm. Fractions that showed UV spectra characteristic of flavonoids were selected and collected.

2.4. Pup mortality

As a first approach to assessing a putative protective effect of quercetin on perinatal asphyxia in the rat model, we determined the number of pups that died 24 h after reanimation in 17 litters subjected to perinatal asphyxia and in 12 litters delivered under control conditions. Pups within each litter were treated either with quercetin or vehicle, as previously described. We analyzed pups' mortality using a mixed-effects logistic regression (using the lme 4 package in R version 3.5.1), considering mortality as the response (binomial variable: 0 = alive and 1 = death) and delivery procedures (S or H), treatment (V or Q) and their interaction as fixed effects. We included the litter (where the pups came from) as a random effect. The best model was selected using the likelihood ratio test.

2.5. Proteomic analyses

2.5.1. Two-dimensional electrophoresis in piglet samples

2.5.1.1. Protein extraction. For the piglet differential proteome study, we used cortex samples from sham-lesioned (SV), hypoxia (HV), and hypoxia treated with 10 mg/kg quercetin nanoliposomal preparation (HQ) groups (n = 4). Protein extraction was performed from approximately 30 mg of fresh tissue samples.

2.5.1.2. Two-dimensional electrophoresis. We prepared 200 μg samples, and the final volumes were adjusted to 125 μl with rehydration buffer (8 M urea, 2% CHAPS, 0,002% bromophenol blue). IPG buffer was added to reach a final concentration of 0.5%, and DTT for a final concentration of 2.8 mg/ml. The sample/rehydration buffer mix was applied to ceramic strip holders (Amersham-Biosciences). A 7 cm 3–10 NL IPG dry strip was added to each sample solution placing the strip with the gel side facing down. The strip was covered with mineral oil. The strip holder was placed in an Ettan IPGphor II Isoelectric Focusing System (GE Healthcare) and subjected to active rehydration at 50 μA/strip for 12 h. Strips were focused as follows: linear increase from #V to 150 V in 30 min, a constant phase of 300 V for 1 h, linear gradient from 300 V to 1000 V for 1 h, linear gradient from 1000 V to 5000 V during 90 min and final constant phase of 5000 V during 6 h. After the first-dimensional separation, IPG strips were removed and reduced for 15 min in an equilibration buffer (75 mM Tris-HCl, pH 8.8, 6M urea, 2% SDS, 30% glycerol, 0.002% bromophenol blue) containing 2% DTT, followed by alkylation for 15 min equilibration in the same buffer containing 25 mg/ml iodoacetamide.

Strips were then rinsed in 1X Tris-Glycine-SDS running buffer and placed in an IPG gel well with the positive end of the strip on the left side of the gels. They were covered with molten overlay agarose at 0,5%. Proteins were then separated in second-dimension on 12% SDS-PAGE in a vertical electrophoresis unit at a constant current of 25 mA per gel at 4 °C until the dye front reached 0.5 cm above the bottom of the gel. The gels were fixed in a mixture of 40% vol/vol ethanol and 10% vol/vol glacial acetic acid for 1 h with continuous gentle shaking and then silver-stained to visualize protein spots. Analysis of the images was done using Image J (https://imagej.net/Fiji; Schindelin et al., 2012) and Melanie 6.0 Software. Quantitative differences in protein expression levels were checked with one-way analysis of variance (ANOVA) with Tukey post-hoc test comparing all group pairings. Protein spots were selected under the following criteria: p values ≤ 0.05 together with a fold-change greater than 1.2.

2.5.2. DIGE in rat samples

2.5.2.1. Protein extraction. Protein was extracted from brain samples dissected 5 h after the cesarean section, from 4 different animals (biological replicates n = 4) for each of the conditions: SV, HV and HQ. The tissues extracted were homogenized in 200 μl of lysis buffer (40 mM Tris base, 7 M urea, 2 M thiourea, 4% CHAPS, 1 mM PMSF, 1% protease inhibitor cocktail Sigma Aldrich #P2714). To remove insoluble

components, the homogenate was centrifuged for 30 min at 4 °C at 14000 g. After centrifugation, the supernatant was transferred to a new reaction tube and stored at −80 °C. These protein homogenates were precipitated using the 2D Clean-up kit (GE Healthcare) according to the manufacturer's instructions. Protein concentration was determined by the Bradford Assay.

2.5.2.2. 2D- DIGE (two-dimensional difference gel electrophoresis). Sample labeling was performed with CyDye™ DIGE Fluor fluorescent probes, Minimal Labeling Kit GE Healthcare (# 28-9345-30), according to the manufacturer's instructions. The pH of the samples was adjusted to 8.5 and these were labeled using 400 pmol of dye for every 50 μg of protein. An internal standard was included in each gel, for which 25 μg of each of the 12 samples were pooled to generate 300 μg of the internal standard which was labeled with CyDye DIGE Fluor Cy2 minimal dye. A Dyeswapping strategy was used to avoid any labeling bias. Two samples labeled with different probes were run on each gel, together with the internal standard labeled with the third dye.

The first-dimension run of the two-dimensional electrophoresis was performed on Immobiline DryStrip strips from GE Healthcare (# 17123501) with a non-linear pH 3–10 range and 18 cm long. After passive rehydration with rehydration buffer (Urea 7 M, thiourea 2 M, chaps 2%) supplemented with IPG buffer 3–10 NL (0.5%) and 20 mM DTT at room temperature, overnight, the isoelectric focusing run was carried out on the Ettan IPGphor II Isoelectric Focusing System (GE Healthcare), under the following conditions: 1. a constant phase of 500 V for 1 h; 2. a linear gradient from 500 V to 1000 V for 1 h; 3. an additional linear gradient from 1000 V to 8000 V for 3 h; 4. and a final constant phase of 8000 V for 90 min. After strips were equilibrated as described above, the electrophoretic run was performed on 12.5% polyacrylamide gels, using the Ettan DALT six system (GE Healthcare Life Sciences) and low fluorescence glasses. The running conditions were as follows: 1) 45 min 2 W/gel at 20 °C; 2) 4 h 17 W/gel at 20 °C. Gels were scanned with a Typhoon FLA 9500 laser scanner (GE Healthcare), at a resolution of 100 μm, using laser wavelengths and filters recommended for each dye. Images were analyzed using the DeCyderTM 2D software (v7.2) (GE Healthcare). The module for Differential In-gel Analysis (DIA) was used for spot co-detection, spot quantification by normalization and calculation of the ratio between different samples in the same gel. Biological Variation Analysis software module was used to perform inter-gel matching and statistical analyses. Student's t-test and one-way analysis of variance (ANOVA) were used to determine whether the standardized spot volume abundance from the samples showed significant changes between conditions. Spots displaying significant volume abundance differences ($p \leq 0.05$) were filtered and selected for further analyses. When different treatments were compared, PCA analysis was used to analyze replicates.

2.5.3. Mass spectrometry

Peptide mass fingerprinting of selected protein spots from both piglet samples in 2D electrophoresis and rat samples in 2D-DIGE was performed by subjecting the samples to in-gel trypsin treatment (Sequencing-grade Promega) overnight at 37 °C. Peptides were extracted from the gels using 60% acetonitrile in 0.2% TFA, concentrated by vacuum drying and desalted using C18- reverse phase micro-columns (OMIX Pipette tips, Varian). Peptides from the microcolumn were eluted directly onto the mass spectrometer sample plate with 3 μl of matrix solution alfa-cyano-4-hydroxycinnamic acid in 60% aqueous acetonitrile containing 0.2% TFA). Mass spectra of digestion mixtures were obtained using a 4800 MALDI-TOF/TOF instrument (Applied Biosystems) in reflector mode and were externally calibrated using a mixture of peptide standards (Applied Biosystems). Collision-induced dissociation MS/MS experiments of selected peptides were performed. Proteins were identified by searching the NCBInr database with peptide *m/z* values using MASCOT software with the following search parameters: monoisotopic mass tolerance, 0.08 Da; fragment mass tolerance, 0.35 Da; methionine oxidation as variable modification, cysteine carbamidomethylation as fixed modification, and one missed tryptic cleavage allowed.

To analyze the respective protein data sets, we performed STRING protein-protein interaction analysis (string-db.org; Szklarczyk et al., 2019) and enriched Gene Ontology (GO) (geneontology.org) analysis to study the biological processes and interactive networks these proteins are involved in.

2.6. Quantitative RT-PCR

Total RNA extraction from sham-lesioned, hypoxia and hypoxia followed by 10 mg/kg quercetin nanosomal preparation (n = 6) piglets' cortex was performed using Illustra RNAspin Mini RNA Isolation Kit (General Electric). Two μg of RNA samples were retrotranscribed using M-MulV Reverse Transcriptase (New England Biolabs) and both OligodT and Random Primers. For Real-time PCR reactions we used the Abi 75000 system (Applied Biosystems), SYBR Green Master mix from Sensimix and specific primers as shown in Table 1. Expression fold changes between groups were calculated according to Pfaffl et al. (2002). Statistical significance in real-time PCR analyses was determined using a permutation-based procedure, the nonparametric pairwise fixed reallocation randomization test, implemented in the Relative Expression Software Tool (REST). P-value < 0.05 was considered statistically significant.

3. Results

3.1. Bioavailability of quercetin in the rat brain

The concentration of quercetin in the brain of neonatal rat pups 30 min after either intranasal or intraperitoneal administration of a nanoliposomal preparation is shown in Fig. 1. We observed that after intranasal administration, quercetin reached the brain with levels similar to those obtained through the previously tested intraperitoneal route of administration (50–100 ng/g of tissue).

3.2. Survival in rats following perinatal asphyxia and quercetin administration

Pup mortality was significantly lower in the group of pups treated with quercetin after perinatal asphyxia. Twenty-four hours after reanimation, 4% (2/49) of vehicle-treated and 0% (0/47) of quercetin-treated Sham pups died. In pups that suffered perinatal asphyxia, mortality was 31% (15/48) in vehicle- and 16% (8/50) in quercetin-treated groups (Fig. 2). The best model predicting pups' mortality includes delivery procedure and treatment as fixed effects and explains 36% of the variance. After including litter as a random effect, the model explains 55% of the variance. Therefore, as shown in Table 2, subjecting pups to the asphyxia procedure during delivery increases their likelihood of dying while receiving quercetin treatment reduces it. These results suggest that quercetin gives protection against death caused by HI injury.

Table 1
Primers used in real-time PCR.

Gene		*5′-3′ primer sequence*
Hif-1-α	Fw	CCTTGGATGGTTTTGTTATGG
	Rev	GCCATTTCTGTGTGTAAGCAT
HO-1	Fw	ATGTGAATGCAACCCTGTGAA
	Rev	GGGAAAGATGCCACAGACTCCT
β-Actin	Fw	CCAGCACGATGAAGATCAAG
	Rev	CAACTAACAGTCCGCCTAGA

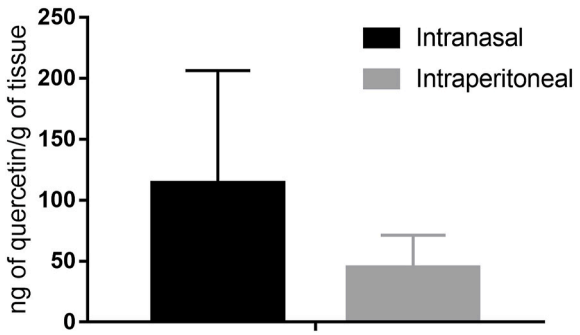

Fig. 1. Quercetin bioavailability. Concentration of nanoliposomal quercetin in ng/g of rat brain tissue after either intraperitoneal or intranasal administration of quercetin (10 mg/kg). Brain samples were collected 30 min after the administration was concluded.

3.3. Changes in gene expression profile after hypoxia and quercetin administration

3.3.1. Expression level of HIF-1α and HO-1 in the piglet

In a previously characterized piglet model, we asked ourselves whether transcription factors and enzymes which were described as master neuroprotective molecules would change with quercetin administration, probably regulating the expression of several other gene products.

Levels of HIF-1α mRNA in the piglet cortex decreased 8 h after asphyxia and reoxygenation (HV), but seemed to be higher in the group treated with quercetin (HQ) as shown in Table 3. HIF-1α mRNA levels almost duplicated when asphyctic animals were treated with quercetin, reaching values similar to those of the sham group.

We also analyzed levels of HO-1, an important target of Nrf2 regulation and crucial in the nervous system response to hypoxic injury. HO-1 mRNA expression clearly increased in HV piglets compared to control sham animals and was significantly lower in the HQ group (quercetin-treated asphyctic animals). Levels in the HQ group were lower (though not statistically significant) than those of sham animals exposed only to vehicle (SV) (Table 3) suggesting that quercetin treatment could not fully recover normal HO-1 levels. We observed the same effect of quercetin in HO-1 levels in other regions as the hippocampus and striatum (data not shown).

3.3.2. Changes in cortex gene expression profile

To identify still unknown pathways or specific proteins that support and explain quercetin neuroprotective action, we performed a large-scale profiling analysis.

3.3.2.1. Gene expression profile in piglet cortex using 2D electrophoresis.

Table 2
Effect of quercetin on pups' mortality. Estimation is based on the number of pups that died 24 h after reanimation in 17 litters subjected to perinatal asphyxia (hypoxia) and in 12 litters delivered by control C-section. Pups within each litter were treated with either quercetin or vehicle, as previously described.
Summary of fixed effect coefficient estimates of the mixed-effects logistic regression model. Mortality was considered the response (binomial variable: 0 = alive and 1 = death); delivery procedures (Sham/control cesarean (S) or Hypoxia/perinatal asphyxia protocol after cesarean delivery (H)), treatment (Vehicle/empty nanoliposomes (V) or Quercetin (Q)) and their interaction were considered fixed effects. N = 193. Estimates are on the logit scale. Asterisks indicate **p < 0.01 and *p < 0.05.

	Estimate	Stand.Error	z value	p
Intercept	−3.99	0.95	−4.19	<0.001**
Hypoxia	3.06	0.99	3.09	0.002**
Quercetin	−1.13	0.54	−2.12	0.03*

Table 3
Quantitative RT- PCR analysis of gene expression of HIF-1α and HO-1 in piglets. Comparison is expressed as the fold change between two conditions. Values were calculated using REST (Relative expression software tool), and p < 0,05 was considered statistically significant.

Gene	Group	Fold change	p
HIF-1α	HV vs SV	0.487	0.010
	HQ vs HV	1.857	0.163
	HQ vs SV	0.904	0.784
HO-1	HV vs SV	2.359	0.072
	HQ vs HV	0.205	0.003
	HQ vs SV	0.482	0.075

SV, Sham-lesioned: no asphyxia protocol/administration of empty nanoliposomes.
HV, Hypoxia: hypoxia-reoxygenation protocol/administration of empty nanoliposomes.
HQ, Hypoxia and quercetin: hypoxia-reoxygenation protocol/administration of quercetin nanoliposomes preparation.
Samples were collected from brain cortex, 8 h after the beginning of hypoxia.

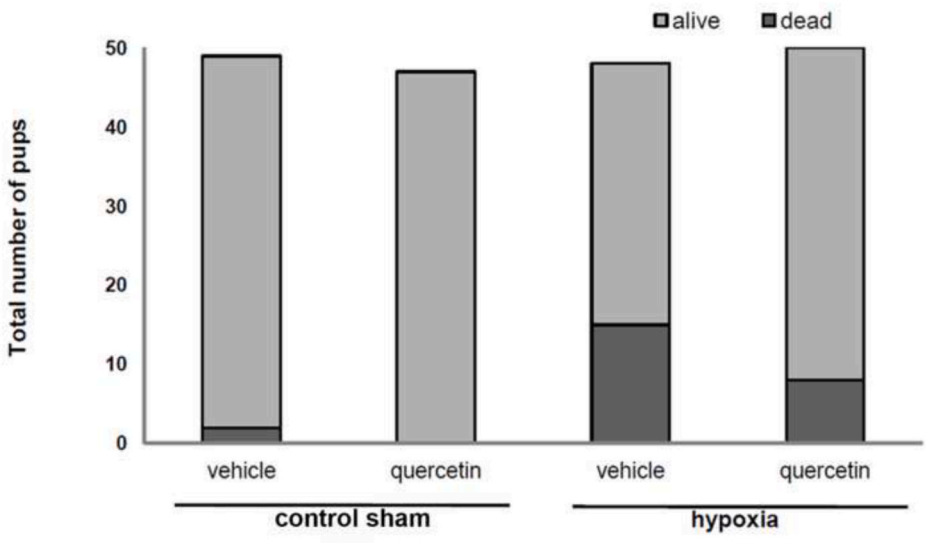

Fig. 2. Survival in rats following perinatal asphyxia and quercetin administration.
Number of surviving and deceased rat pups 24 h after the asphyxia protocol followed by intraperitoneal injection of either a quercetin preparation or vehicle alone. Bars represent proportion of deceased and surviving pups in each experimental group: Sham (delivered by cesarean) and administered vehicle (SV) or quercetin (SQ); vehicle-treated (HV) or quercetin-treated pups (HQ) after perinatal asphyxia.

To assess the magnitude of the changes in relative protein abundance in the piglet cortex proteome after hypoxia and quercetin treatment, we performed two-dimensional electrophoresis. We observed 34 protein spots that changed their relative abundance in the different treatment groups. Seventeen spots, whose intensity under hypoxia or quercetin treatment changed with respect to sham, were identified by MALDI-TOF MS (Table 4). Two of them (enolase-1 and triosephosphate isomerase) showed differences in pI, and one spot corresponding to fructose-biphosphate aldolase A was exclusive to quercetin treated group. These proteins were not included in quantification analysis, but are considered changing proteins (Fig. 3).

Protein spots were classified in three groups according to spot intensity and differential expression profile (Table 4). The first group consisted of proteins whose abundance increased under hypoxia and quercetin treatment (HQ) compared to sham or hypoxia groups. This group included NADH dehydrogenase ubiquinone flavoprotein 2 mitochondrial, Glutathione S-transferase P, voltage-dependent anion-selective channel protein 1 (VDAC1), cofilin-1 and acidic leucine-rich nuclear phosphoprotein 32. The second group included those proteins that changed under hypoxia treatment and remained altered after quercetin treatment, such as complement component 1 Q subcomponent-binding protein, glial maturation factor-beta, phosphatidylethanolamine-binding protein 1, and aldolase C, fructose-bisphosphate. The third group consisted of proteins that showed a change in abundance under hypoxia but reverted to initial levels after quercetin treatment. This group included superoxide dismutase 1 and stathmin wich increased their levels under hypoxia, and beta-actin whose levels decreased under hypoxia. We interrogated the String database for interactions and associations between the proteins identified in this study. Eight of the 17 identified proteins showed interactions, in many cases supported by more than one type of evidence (Fig. 4). Enzymes that participate in the glycolytic pathway belong to one association group, and proteins linked to oxidative stress to another.

Statistical enrichment tests were performed to find significant over-represented GO and InterPro categories. Proteins identified using Panther GO were found to be mainly associated with catalytic activity and binding functions, in accordance with String results. Metabolite interconversion enzymes are a predominant class of proteins. The glycolytic pathway is represented along with other signaling pathways.

3.3.2.2. Difference in protein relative abundance in rat cortex using 2D DIGE. The rat model study involved a more sensitive method such as two-dimensional difference gel electrophoresis (2D-DIGE). This technology allows for simultaneous direct comparison of changes in protein abundance across multiple samples, without interference due to gel-to-gel variation. An average of 2370 spots was resolved in each gel using this approach (Fig. 5). Changes in abundance of protein spots were measured as volume ratios, and a total of 161 differential spots were selected. Among those differential expressed spots, 43 were revealed in the Coomassie Brillant Blue-stained gels and excised for subsequent mass spectrometry and database interrogation. Table 5 shows 27 protein spots that could be identified as corresponding to 22 unique proteins. The average ratios were calculated by comparing the volume of each spot in one condition with that of the corresponding spot for the other condition (Sham vs. hypoxia, HV/SV; Sham vs. quercetin, HQ/SV; hypoxia vs. quercetin, HQ/HV).

Several proteins were identified in more than one spot, although they were excised from the same gel. This was the case with heat shock 70

Table 4
Selection of piglet proteins with differential expression.
List of proteins identified by MALDI-TOF/TOF MS HV/SV (Hypoxia vs. Sham), HQ/SV (Hypoxia plus quercetin treatment vs. Sham) and HQ/HV (Hypoxia plus quercetin treatment vs. Hypoxia plus vehicle) columns show the comparison expressed as fold changes between two experimental conditions with averaged expression values from each spot in 3–4 gel technical replicates.
The "-" sign indicates down-regulation. The "*" symbol indicates that this Mascot score corresponds to the MS/MS ion score of the unique peptide identified for Beta actin. Only fold change values that were statistically significant ($p < 0.05$) are shown. Theoretical and observed MW and pI are indicated. Accession numbers correspond to NCBI protein entries. Percentage of coverage and number of peptides matched are also shown. Proteins were classified in three groups according to their changing profiles. Group 1: proteins that significantly increased their expression under hypoxia and quercetin treatment (HQ) compared to sham (SV) or hypoxia (HV) (spots 1 to 5), Group 2: proteins that significantly changed under hypoxia and remained altered after quercetin treatment (spots 6 to 9), and Group 3: proteins that showed a change in expression under hypoxia but reverted to initial levels after quercetin treatment (spots 10 to 12).

		Fold change							
Spot number	**Name**	**HV/SV**	**HQ/SV**	**HQ/HV**	**Accession number**	**Mascot score**	**Peptides matched**	**MW Theor/Obs**	***pI* Theor/Obs**
1	Acidic leucine-rich nuclear phosphoprotein 32 family member A		1.42	1.28	XP_003121807.3	125	3	28.5/30.0	4.0/4.8
2	Cofilin-1		1.62	1.70	NP_001004043.1	125	6	18.5/20	8.2/6.0
3	NADH dehydrogenase ubiquinone flavoprotein 2, mitochondrial		1.58	1.38	NP_001090944.2	130	10	25.5/25.0	6.9/6.0
4	Glutathione S-transferase P		1.36	1.45	P80031.2	117	4	21.6/25.0	7.1/5.8
5	Voltage-dependent anion-selective channel protein 1		1.60	1.83	NP_999125.1	184	9	30.7/33.0	8.6/6.0
6	Aldolase C, fructose-bisphosphate	−1.33	−1.47		NP_001230857.1	255	17	39.3/45.0	6.2/6.0
7	Glia maturation factor beta	1.92	1.64		NP_001231390	127	4	16.7/45.0	5.1/5.5
8	Complement C1q binding protein, mitochondrial	1.23	1.28		XP_020923404.1	112	8	28.8/30.0	4.7/4.8
9	Phosphatidylethanolamine-binding protein 1 isoform X1	1.20	1.20		XP_003132938.1	165	4	20.9/25.0	6.9/6.0
10	Superoxide dismutase 1	1.20		−1.37	NP_001177351.1	166	6	15.2/12.0	6.0/5.8
11	Stathmin	1.30	−1.25	−1.61	NP_001009582.1	161	6	17.3/20.0	5.7/5.4
12	Beta actin	−1.20		1.22	AAS55927.1	66*	1	44.7/50.0	5.3/5.7
13	Enolase 1			*pI* change	XP_020950937.1	249	11	61.4/55.0	10.4/5.8
14	Enolase 1			*pI* change	XP_020950937.1	180	10	61.4/55.0	10.4/5.5
15	Triosephosphate isomerase 1			*pI* change	BAI48105.1	242	12	26.6/27.0	6.5/5.5
16	Triosephosphate isomerase 1			*pI* change	BAI48105.1	141	8	26.6/27.0	6.5/6.0
17	Fructose-bisphosphate aldolase A		exclusive to HQ		XP_020943655.1	147	10	39.4/45.0	8.4/6.3

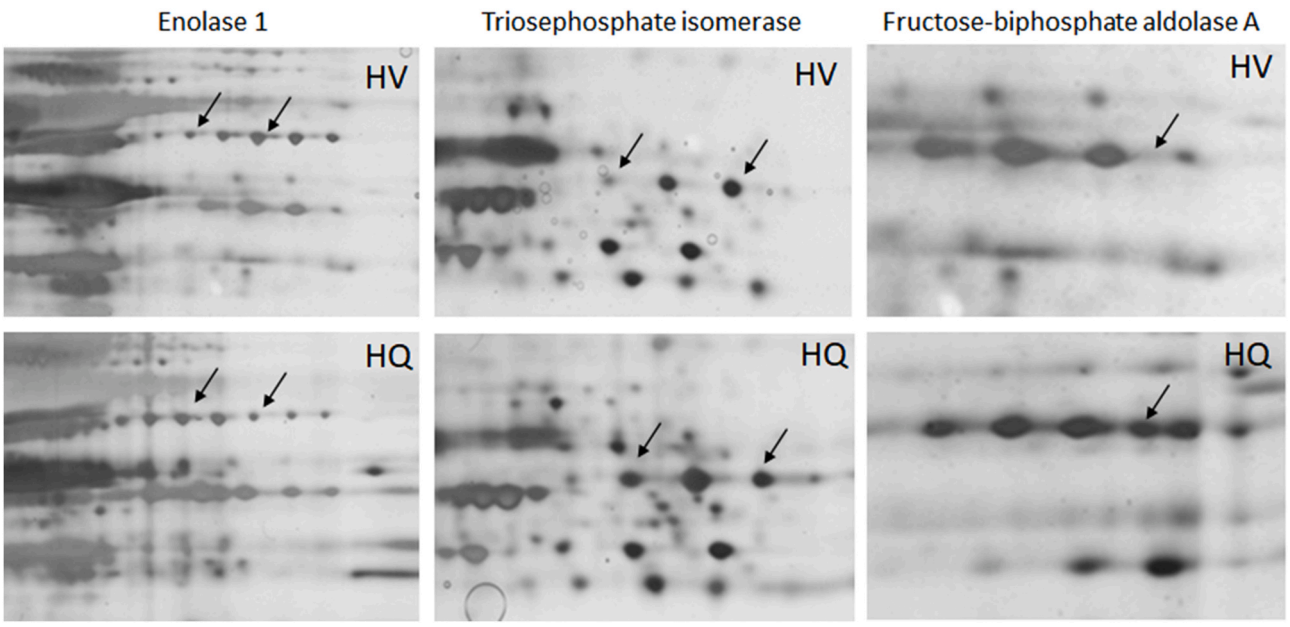

Fig. 3. Piglet proteoforms identified by two-dimensional electrophoresis analysis. Gel images show changes in the isoelectric point (arrows) for alpha-enolase (left) and triosephosphate isomerase (center), when comparing HV with HQ samples. Gel images on the right show a proteoform of fructose-biphosphate aldolase A exclusive to quercetin-treated samples HQ compared to HV (right). HV and HQ represent vehicle-treated and quercetin-treated after perinatal asphyxia.

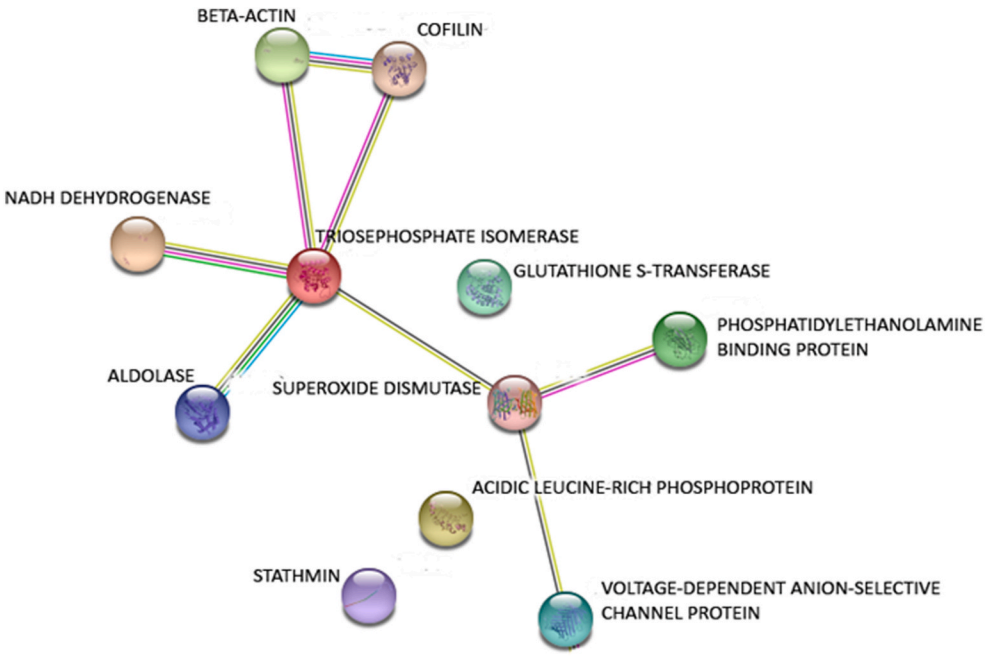

Fig. 4. Newborn piglet proteins identified as differentially expressed by 2D electrophoresis. Protein data set was identified by network analysis using STRING (Search Tool for Recurring Instances of Neighbouring Genes) software.

kDa protein 4, serotransferrin, transketolase and POTE ankyrin domain family member F isoform X2. Proteins present in more than one spot could be proteoforms, perhaps due to post-translational modifications.

When we interrogated the databases to identify interactions and associations, we found several proteins related to metabolism among those proteins that change significantly. String analysis showed that there were more significant interactions between identified proteins than expected by chance (Fig. 6) which were mainly associated with "response to stimulus" and "response to stress" in biological process (GO) terms enrichment analysis and with "ion binding" and "protein binding" in molecular function (GO) terms enrichment analysis (Table 1S). KEGG analysis showed that tight junction and AMPK and HIF-1 signaling pathways were overrepresented.

4. Discussion

Therapeutic hypothermia is the current standardized neuroprotective treatment strategy to improve recovery of HIE (Ahearne et al., 2016; Gluckman et al., 2005). However, a lot of research is aimed at designing adjuvant therapies to improve neurological outcomes of newborns with HIE (McAdams and Juul, 2016).

The aim of this study was to obtain further molecular evidence on the

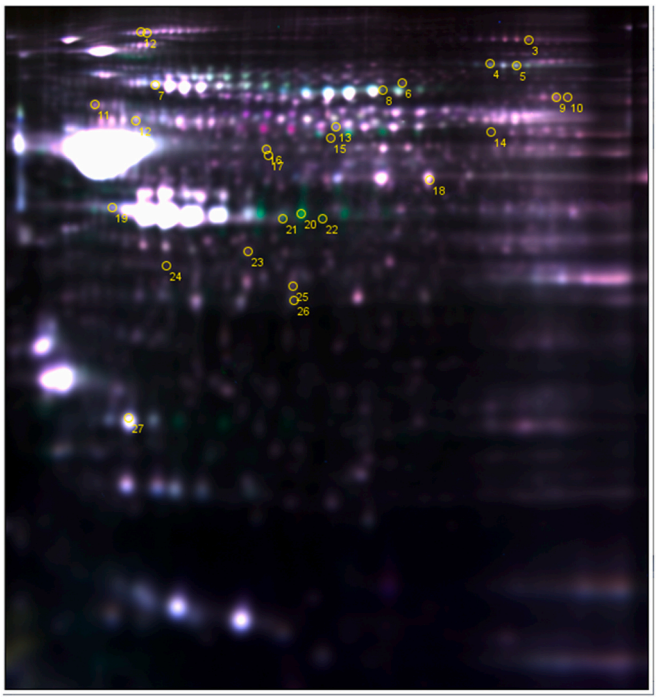

Fig. 5. Representative two-dimensional difference with a sample from the HQ group (red dye) and a sample from the SV group (blue dye), and internal control pool (yellow dye). Yellow circles and corresponding numbers indicate spots that presented significant expression changes. Spot numbers correspond to those listed in Table 5.

neuroprotective activity of quercetin through the identification of specific targets and pathways implied in its action. The use of two animal models allowed us to better study and understand the changes in gene expression. Despite their differences regarding brain development, quercetin administration route and time of sampling, both models provided a picture of the main protein changes that occur after a severe hypoxic injury and quercetin administration.

4.1. Quercetin bioavailability and protective effect

The therapeutic success of neuroprotective compounds depends on accurate information about routes of administration and drug bioavailability. As a novel report, in this work, the administration of the nanoliposomal preparation of quercetin by either intranasal or intraperitoneal route in newborn rats increased quercetin brain levels 30 min after administration. In particular, the intranasal administration proved to be an efficient route for this nanoliposomal preparation. Quercetin levels in rat cortex samples are in accordance with those previously reported in piglets after the intravenous administration of the same preparation (Blasina et al., 2015). Díaz et al. (2015) confirmed the neuroprotective capacity of nanosomes of quercetin in an experimental rat model of Parkinson's disease with measurable levels of quercetin in the brain after either intraperitoneal or intravenous injection of the same quercetin preparation.

A detailed study is necessary, however, since differences in dosing between routes and timing of administration of the drug will most likely influence not only the maximum concentration of quercetin that reaches the brain but also its pharmacokinetics. Data from our group (data not shown) indicate that maximum quercetin concentration in the brain when administered through the intraperitoneal route is probably obtained as soon as 15 min after administration. Nonetheless, the intranasal route could have some advantages in a future clinical setting, in terms of low complexity of the procedure for administration and might allow the preparation to reach the brain more directly (Kumar et al., 2017). Recent research has also analyzed the applicability of intranasal quercetin administration for Alzheimer's disease treatment (Agrawal et al., 2018) and cerebral ischemia (Ahmad et al., 2018). However, even if intranasal administration is promising, a higher dose should be considered, perhaps in a more concentrated preparation.

We found that in neonatal rats subjected to the immersion protocol, quercetin increased survival with protective effects, made apparent by changes in mortality and gene expression. These results suggest that a single 10 mg/kg dose of nanoliposomal preparation reached hypoxic-ischemic affected tissues having a beneficial *in vivo* effect which is valuable in defining a therapeutic dose. This is consistent with the results by Lei et al. (2015) that reported nearly 80% survival with a repeated oral administration. Brain concentrations of 50–100 ng/g are similar to those found by other authors (Ahmad et al., 2018; Rivera et al., 2004). Besides, as HIE related to perinatal asphyxia is currently unpredictable, a suitable treatment must be one that confers protection against brain injury when administered after the insult. In this sense, the present result in the rat model along with previous evidence in the piglet model (Blasina et al., 2015) suggest that with a single administration of quercetin after asphyxia the nanoliposomal quercetin treatment is a good putative tool for clinical use. Nevertheless, it would be valuable to assay repeated doses of quercetin through any of the routes to explore if it enhances the protective action.

4.2. Targets of quercetin for neuroprotective action

It was reported that treatment with quercetin may exert a protective effect against oxidative damage by direct and indirect antioxidant pathways (Dajas et al., 2015) and prevent the loss of pyramidal neurons from the hippocampus in ischemia-reperfusion induced in rats (Ghosh et al., 2013). An antiapoptotic effect has also been reported (Ossola et al., 2009; Sharma et al., 2016; Srivastava et al., 2016). However, although its multitarget capacity has been described, the exact mechanism of the neuroprotective effect of quercetin against global brain injury has remained elusive.

4.2.1. Quercetin action on HIF1-α and HO-1

In order to deeply explore the therapeutic value of quercetin, we first analyzed its action on two well-known genes related to response to hypoxic and oxidative stress, and afterward undertook a proteomic approach. The current approach was focused on cortex gene expression. Ara et al. (2011) described during HI injury in the newborn piglet model, that most of the neuronal loss was observed in the cortex and underlying white matter followed by hippocampus and striatum. The basal ganglia, cerebellum, and thalamus were affected to a lesser extent. Likewise, in the rat model the cortex has a great postnatal maturation that makes it particularly sensitive to this kind of damage (Kletkiewicz et al., 2018). Consistent with this evidence, we found that perinatal asphyxia modified gene expression in the cerebral cortex of both species analyzed.

We analyzed HIF-1α, a transcription factor that plays a fundamental role as regulator of oxygen homeostasis under hypoxic conditions by regulating gene expression (Semenza, 2004). We observed that HIF-1α mRNA levels significantly decreased in asphyctic piglets and almost duplicated when animals were treated with quercetin, reaching values comparable to those in sham groups. Several authors have reported accumulation of HIF-1α m RNA or protein under hypoxic conditions, while several other studies provided evidence that HIF-1α mRNA is not upregulated (Wenger et al., 1997), and in some other cases, although upregulated during hypoxia, a quick drop to basal levels following reoxygenation is observed. Furthermore, the presence of an antisense HIF RNA can promote HIF mRNA degradation (Poitz et al., 2014). Kirova et al. (2013) proposed that features of HIF-1α response to hypoxic exposure depend in part on severity and duration of hypoxia insult. Thus, induction optimally occurs only within a limited range of oxygen concentrations in the inspired air (18-10% O2). Reduced oxygen concentration in the inspired air to 8% or lower impair the immediate

Table 5
Selected rat proteins identified with differential expression. List of proteins identified by MALDI-TOF/TOF MS. Spot numbers correspond to those in Fig. 5. HV/SV (Hypoxia vs. Sham), HQ/SV (Hypoxia plus quercetin treatment vs. Sham) and HQ/HV (Hypoxia plus quercetin treatment vs. Hypoxia plus vehicle) columns show fold changes of spot volumes calculated as the ratio of the average standardized abundances corresponding to the two conditions. Asterisks represent significant statistical differences ($p < 0.05$). The "-" sign indicates down-regulation. Theoretical MW and pI are indicated. Accession numbers correspond to NCBI protein entries. Percentage of coverage and number of peptides matched also are shown.

Spot number	Name	HV/SV	HQ/SV	HQ/HV	Accession number	Mascot score	Peptides matched	MW	*pI*
1	heat shock 70 kDa protein 4	−1.09	−1.12*	−1.02	NP_705893	283	28	93997	5.12
2	heat shock 70 kDa protein 4	−1.14*	−1.1	1.03	NP_705893	311	29	93997	5.12
3	elongation factor 2	−1.39*	−1.14	1.22	NP_058941	353	32	95223	6.41
4	serotransferrin	1.29*	1.23	−1.06	NP_001013128	264	24	76346	7.14
5	serotransferrin	−1.18	1.09	1.28*	NP_001013128	321	29	76346	7.14
6	dihydropyrimidinase-related protein 2 isoform X1	−1.15	1.06	1.22*	XP_006252159	382	36	73115	5.99
7	heat shock cognate 71 kDa protein	1.18*	1.09	−1.08	NP_077327	317	32	70827	5.37
8	serum albumin	−1,02	1.44*	1.47	P02770	194	17	68686	6.09
9	transketolase, isoform CRA_c	−1.33*	−1.13	1.17	EDL88993	252	16	55745	7.14
10	transketolase, isoform CRA_c	−1.31*	−1.27*	1.03	EDL88993	139	13	55745	7.14
11	serine/threonine-protein phosphatase 2A 65 kDa regulatory subunit A alpha isoform isoform X1	−1.02	−1.21*	−1.19*	XP_007648156	322	27	65038	4.96
12	heterogeneous nuclear ribonucleoprotein K	−1.09	1.16	1.26*	XP_016835931	254	19	48530	5.38
13	dihydropyrimidinase-related protein 3	1.31*	1.31	−1.02	NP_037066	340	25	61928	6.04
14	pyruvate kinase PKM isoform X2	1.13*	1.06	−1.07	XP_006243252	176	13	64484	6.63
15	protein phosphatase 3, catalytic subunit, alpha isoform, isoform CRA_a	−1.03	1.09*	1.13	EDL82280	133	6	42316	5.90
16	V-type proton ATPase subunit B, brain isoform	−1.22*	−1.15	1.06	NP_476561	171	20	56515	5.57
17	tubulin, alpha 1A	−1.3*	−1.58*	−1.21	AAH62238	121	13	50104	4.94
18	alpha-enolase isoform X1	−1.12*	−1.03	1.09	XP_006239506	363	23	47228	5.90
19	POTE ankyrin domain family member F isoform X2	1.23*	1.37	1.11	XP_002725368	318	16	44861	5.62
20	tubulin beta-2B chain	2.79	4.18*	1.50	NP_076205	388	26	49921	4.78
21	POTE ankyrin domain family member F isoform X2	−1.08	1.28	1.38*	XP_002725368	117	8	44861	5.62
22	tubulin beta-3 chain	1.56	2.42*	1.55	NP_075768	251	21	50386	4.82
23	guanine nucleotide-binding protein G(o) subunit alpha isoform X1	−1.08	−1.19*	−1.11	XP_008770543	156	13	39995	5.69
24	serine/threonine-protein phosphatase 2A catalytic subunit alpha isoform	1.16*	1.13	−1.03	NP_058735	101	7	35585	5.30
25	malate dehydrogenase 1, NAD (soluble)	−1.12	1.03	1.15*	AAH59124	98	10	36461	5.92
26	G protein beta 1 subunit	1.08	1.13*	1.05	AAC72249	74	7	37369	5.47
27	POTE ankyrin domain family member F isoform X1	2.46*	3.04*	1.24	XP_002728578	164	6	45903	5.45

oxygen-dependent accumulation of HIF-1α and oxygen-independent synthesis in the neocortex of rats (Kirova y col 2013). In our case, in the piglet model, 8 h after perinatal asphyxia and reanimation, HIF-1α mRNA levels were decreased while quercetin could help to increase levels again. These results support that quercetin can act through the HIF pathway in the newborn cortex. Besides the already known quercetin effect at the post-transcriptional level (Triantafyllou et al., 2007), we describe an effect at the transcriptional level.

Changes in both the expression level and in the intracellular location of the Nrf2 factor in response to quercetin are well documented including previous works in our laboratory (Arredondo et al., 2010). We, therefore, decided to analyze Heme oxygenase-1 (HO-1) levels, an important target of Nrf2 regulation and crucial in nervous system response to damage. Asphyctic piglets exhibited a significant increase in HO-1 mRNA while quercetin-exposed animals had decreased levels. The protective role of HO-1 against oxidative neuronal damage has been confirmed by experiments performed on animal models (Nitti et al., 2018). Particularly, in the case of ischemia, animal exposure to pterostilbene prevents ischemic brain damage in newborns through the Nrf2-dependent induction of HO-1 (Li et al., 2016). It has also been demonstrated that quercetin increases Nrf2/HO-1 favoring neuroprotection against galactose-induced damage (Dong et al., 2017). Our results point in the same direction, since the success of protection through quercetin can be partially explained by up-regulation of HO-1.

4.2.2. *Proteomic profile of neonatal cortex*

In addition to these two proteins with an established connection to neuroprotection in different HI models, we dedicated our efforts to the search for less known targets and pathways affected by quercetin treatment in response to neonatal HI.

Over the last decade, several studies have demonstrated the power of large-scale differential expression analysis of genes and their products in response to ischemia. This approach can provide a large amount of information at once (Van Elzen et al., 2008), and therefore has the potential to uncover clusters of participating proteins with co-regulated expression and, in some cases, shared functionality.

The proteomic approach undertaken in the two models under study showed a set of proteins, some of them hardly ever associated with quercetin, which help to identify new targets and pathways related to its neuroprotective action. In the piglet model, we selected 17 spots from analysis that changed with hypoxia or with hypoxia-quercetin treatment and identified them. Thirteen proteins changed upon hypoxia and 8 were modified by quercetin treatment. We classified them into three classes according to their differential relative abundance in experimental groups. In the first class, we grouped proteins that increased with hypoxia followed by quercetin treatment (HQ) when compared with sham or HV, including proteins related with oxidative stress like Glutathione S-transferase P and several mitochondrial proteins. These proteins could respond to quercetin treatment either because they are direct targets of the compound or because the treatments (hypoxia and then quercetin) secondarily induce its changes. In the second class, we grouped proteins that changed with hypoxia and were not clearly modified by quercetin. In the third group, we included proteins that changed with hypoxia but returned to sham level to a certain extent with the subsequent quercetin treatment, becoming candidates to be targets in the response to quercetin following hypoxia.

String analysis established interactions among identified proteins defining groups related to glycolytic metabolism and oxidative stress.

In group 1 we identified Acidic Leucine-rich nuclear phosphoprotein 32 (ANP32A), a protein not previously related with quercetin whose

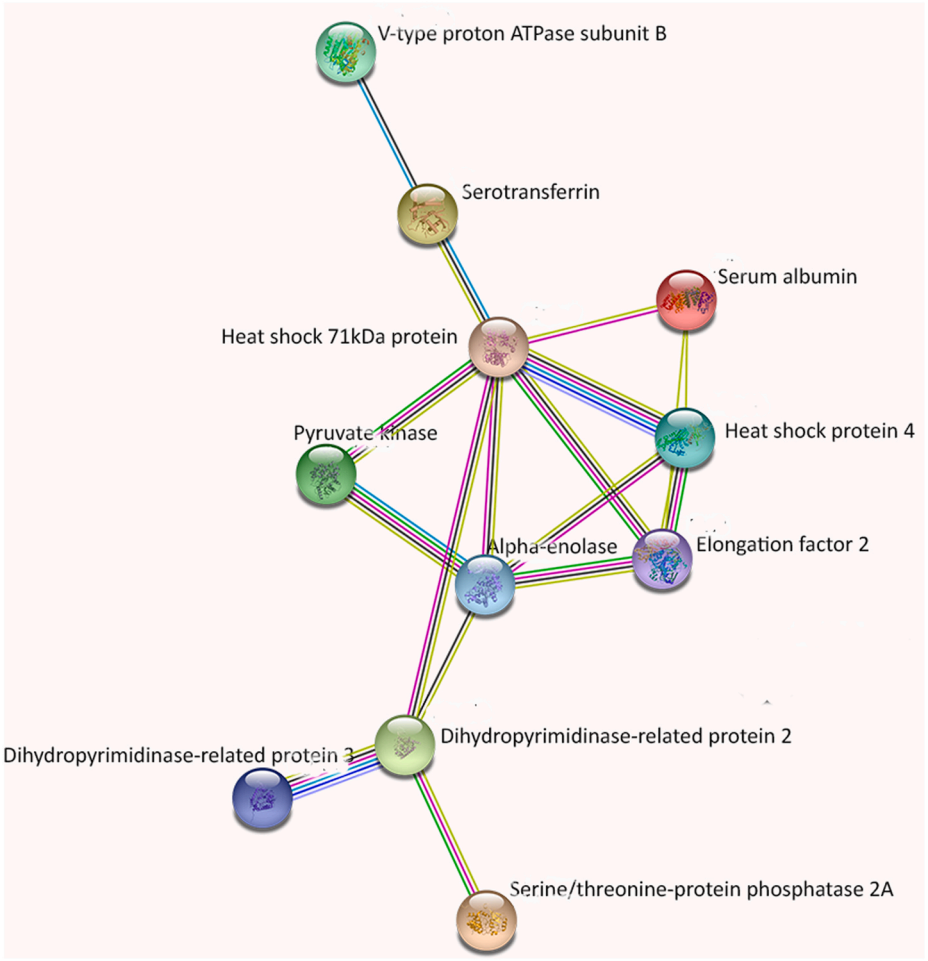

Fig. 6. Newborn rat proteins identified as differentially expressed by DIGE. Protein data set was identified by network analysis using STRING (Search Tool for Recurring Instances of Neighbouring Genes) software.

level is induced in HQ group. In our laboratory, we attained the same effect on mRNA levels by real-time RT-PCR, strongly suggesting that quercetin is contributing to change the expression of this gene. ANP32A regulates RNA stability as well as transport, and may control enzymatic activities by inhibition of protein phosphatase 2A (PP2A) or activation of caspases (Wang et al., 2015). It has also been related to development and differentiation of the nervous system (Kular et al., 2009) on account of its ability to modulate cytoskeletal networks. Furthermore, it mainly operates as a component of the inhibitor of histone acetyltransferase complex in cortical neurons (Kadota and Nagata, 2011), opening the possibility that quercetin, by means of its action on ANP32, could be implicated in chromatin condensation and therefore regulation of transcription of other genes.

On the other hand, three enzymes that participate in the glycolytic pathway of metabolism were identified in our 2D gels with changes in their relative abundance profiles. A unique spot identified as fructose-bisphosphate aldolase A could be detected only upon quercetin treatment. Triosephosphate isomerase 1 and alpha-enolase were seen in rows of spots of the same MW but different isoelectric point, presumably corresponding to distinct proteoforms. Interestingly, one of them, alpha-enolase has been described as a multifunctional protein displaying a range of distinct activities and whose gene carries in its promoter a hypoxia response element (Semenza et al., 1996).

Several proteins in groups 1 and 3, affected by quercetin are also known targets of the Nrf2 pathway, as glutathione S-transferase (GST) and SOD-1 (Shih et al., 2005; Zhang et al., 2010). These changes could be directed to stabilize metabolism and recover cells from energy failure, increasing the expression of the complete battery of glycolytic enzymes (Lee et al., 2007). As some cells failed to recover, they must be redirected to death pathways, which may explain why proteins like VDAC1 and cofilin 1 increased with quercetin administration (Alhadidi and Shah, 2018; Shoshan-Barmatz et al., 2018). The latter was recently proposed as a promising therapy for different brain injury mechanisms.

Results in DIGE proteomic approach in newborn rats confirmed some previous results in piglets as proteins related to metabolism were again represented. GO classes showed that in both models, proteins with catalytic activity were the most represented. Proteins such as pyruvate kinase, malate dehydrogenase and enolase changed their levels with hypoxia in rats. In all these cases, levels were similar to sham after quercetin treatment. Alpha enolase levels that were significantly decreased in asphyctic pups, were like sham in the group treated with quercetin. This protein also changed its profile in the piglet model showing an isoelectric point change in asphyctic animals and recovering with quercetin. Enolase can be converted to neuron-specific enolase (NSE), a glycolytic enzyme found in neuronal and neuroendocrine tissues that may play a dual role in promoting both neuroinflammation and neuroprotection. It could be a marker of neuronal injury but may also show neurotrophic function as it controls neuronal survival, differentiation, and neurite regeneration (Haque et al., 2018), and has been identified as a marker in previous studies of asphyxia models (Weitzdörfer et al., 2008).

As our goal was to describe the multitarget nature of quercetin and to identify new targets, it is worth taking notice of other rat proteins that we found related to each other in the enrichment analysis of STRING

consortium. Noteworthy among them are more than one isoform of dihydropyrimidinase-related protein and subunits of protein phosphatases.

Dihydropyrimidinase-related protein 2 (Dpys2), also known as Collapsin response mediator protein 2 (CRMP2), has been related to polarization, neural differentiation and axonal growth (Shah et al., 2018), and inhibits the generation of p53-induced apoptotic genes (Llanos et al., 2006; Suzuki et al., 2003). In the rat model in the present study, Dpys2 is induced with quercetin. Shah et al. (2018) have recently shown that melatonin, with a neuroprotective role, increased levels of CRMP2 in a middle cerebral artery occlusion (MCAO) model. Our results point in the same direction, and, as this protein can be altered by phosphorylation and by cleavage, further investigation must be done to confirm its behavior in perinatal asphyxia and a putative role of quercetin in its modifications.

Three subunits of phosphatases were also identified in rat proteome profiling: two phosphatase 2A subunits and one phosphatase 3 subunit. Serine/threonine protein phosphatase 2A has multiple biological activities from cellular metabolism to development and apoptosis being an important component in the dephosphorylation process (Bennecib et al., 2000; Liu et al., 2005). Shah et al. (2015) has found it downregulated in the cortex 24 h after MCAO. Our study demonstrated an increase in catalytic subunit after hypoxia injury, unrecovered by quercetin administration. However, we also found decreased expression of regulatory subunit after quercetin treatment both with respect to SV and to HV pups, suggesting that with quercetin administration this complex holoenzyme is being finely tuned. PP2A is described to achieve substrate specificity and regulation through combinatorial interactions between conserved catalytic subunits and a large number of regulatory subunits (Shi, 2009). It would be important therefore to further analyze the effective change in this phosphatase's activity in the rat model. If a decreased activity could be demonstrated after quercetin treatment we could hypothesize that, as was described for propofol protective action (Zhu et al., 2015), a decrease in PP2A expression could control endothelial inflammation induced by HIE. On the other hand, as addressed by Kruse et al. (2020), the regulatory subunit affects the phosphorylation site preference of the holoenzyme catalytic subunit, suggesting that quercetin could be redirecting phosphatase activity to different substrates. Interestingly, in the piglet model, we found that quercetin increased ANP32A protein, known to inhibit this phosphatase.

In our study in rats, several proteins of the family of proteins with ankyrin domain changed their expression pattern. This family has been previously shown to be involved in regulating the amount of factor inhibiting HIF (FIH) available to hydroxylate HIF-1α and hence, the level of this transcription factor (Yang et al., 2011).

We have also found that quercetin significantly increased the level of Heterogeneous nuclear ribonucleoprotein K (hnRNPK), found to be involved in the maintenance of ATP levels upon cellular stress (Fukuda et al., 2009). There is strong evidence that hnRNP K plays an important role in the post-transcriptional regulation of multiple genes involved in the cytoskeletal organization of axons (Liu and Szaro, 2011). In addition, it interacts with glycogen synthase-3β (GSK3β) mRNA, regulating various signaling pathways. Particularly, the phosphorylation of the protein Dpys2 also found in this report is mediated by GSK3 beta. A decrease in the level of another heterogeneous nuclear ribonucleoprotein, hnRNPD, has been described in the same asphyxia model used in our report (Weitzdörfer et al., 2008). Moreover, specific interaction was described between the member hnRNPA1 and quercetin resulting in its cytoplasmic retention (Ko et al., 2014). These pieces of evidence suggest the importance of this family of proteins in a putative protective role.

In summary, research in neuroprotective pharmacology aims to identify forceful compounds to further reduce and repair damage to the immature brain after perinatal asphyxia, which functions as a synergic complement to hypothermia treatment. We consider quercetin a serious candidate to advance in clinical trials. Nanoliposomal preparation available through different administration routes, reached effective concentrations modulating the expression of proteins involved in energy metabolism, homeostasis, axonal growth and oxidative response in the cortex. A more in-depth understanding of the contribution of proteins such as CRMP2, enolase, hnRNPK or PP2A could bring valuable insight regarding the mechanisms responsible for the neurological disabilities frequently observed in HIE newborns and the complex action mechanisms of quercetin, contributing to the design of effective therapies to this severe illness.

Funding

This work was supported in part by the Agencia Nacional de Investigación e Innovación (ANII), Uruguay [POS_NAC_2015_1_109509 and INI_X_2011_1_3894], Comisión Sectorial de Investigación Científica (Universidad de la República, Uruguay) and PEDECIBA (Programa de Desarrollo de Ciencias Básicas) and PROINBIO, UdelaR.

The funding source(s) had no involvement in any decision related with this research or preparation of manuscript.

Acknowledgments

The authors wish to thank Hector Rodriguez for the excellent care of the rats, José Barreto for his assistance during piglet experiments and Granja La Familia for piglet breeding. We also thank Dr. Ivan Gonzalez-Bergonzoni for statistical analysis, Lucía López and Ileana Sosa for their assistance during asphyxia protocol in rats, and Juan Andrés Abin and Marcela Martínez for their help in HPLC analysis at IIBCE, Montevideo, Uruguay.

Appendix A. Supplementary data

Supplementary data to this article can be found online at https://doi.org/10.1016/j.neuint.2021.105064.

Author contributions

Cardozo, Viviana: Conceptualization, Methodology, Formal Analysis, Investigation, Writing- Original draft preparation Parodi-Tálice, Adriana: Conceptualization, Methodology, Validation, Formal Analysis, Investigation, Data curation, Writing- Original draft preparation Vaamonde, Lucía: Methodology, Validation, Investigation, Resources, Writing- Original draft preparation Zuluaga, María José: Methodology, Investigation Agrati, Daniella: Methodology, Validation, Resources Lima, Analía: Formal Analysis Portela, Madelón: Formal Analysis Blasina, Fernanda: Conceptualization, Methodology, Validation, Investigation, Resources, Writing- Original draft preparation, Writing - Review & Editing Dajas, Federico: Writing - Review & Editing Bedó, Gabriela: Conceptualization, Methodology, Validation, Investigation, Writing- Original draft preparation, Writing - Review & Editing.

Declaration of interests

The authors declare that they have no known competing financial interests or personal relationships that could have appeared to influence the work reported in this paper.

References

Agrawal, M., Saraf, S.S.S., Saraf, S.S.S., Antimisiaris, S.G., Chougule, M.B., Shoyele, S.A., Alexander, A., 2018. Nose-to-brain drug delivery: an update on clinical challenges and progress towards approval of anti-Alzheimer drugs. J. Contr. Release 281, 139–177. https://doi.org/10.1016/j.jconrel.2018.05.011.

Ahearne, C.E., Boylan, G.B., Murray, D.M., Ahearne, C.E., Boylan, G.B., Murray, D.M., Yn, C.T., Ahearne, C.E., Boylan, G.B., Murray, D.M., 2016. Short and long term prognosis in perinatal asphyxia: an update. World J. Clin. Pediatr. 5, 67–75. https://doi.org/10.5409/wjcp.v5.i1.67.

Ahmad, N., Ahmad, R., Naqvi, A.A., Alam, M.A., Ashafaq, M., Abdur Rub, R., Ahmad, F. J., 2018. Intranasal delivery of quercetin-loaded mucoadhesive nanoemulsion for

treatment of cerebral ischaemia. Artif. Cells, Nanomedicine Biotechnol 46, 717–729. https://doi.org/10.1080/21691401.2017.1337024.
Alhadidi, Q., Shah, Z.A., 2018. Cofilin mediates LPS-induced microglial cell activation and associated neurotoxicity through activation of NF-κB and JAK–STAT pathway. Mol. Neurobiol. 55, 1676–1691. https://doi.org/10.1007/s12035-017-0432-7.
Ara, J., Fekete, S., Frank, M., Golden, J.a, Pleasure, D., Valencia, I., 2011. Hypoxic-preconditioning induces neuroprotection against hypoxia-ischemia in newborn piglet brain. Neurobiol. Dis. 43, 473–485. https://doi.org/10.1016/j.nbd.2011.04.021.
Arredondo, F., Echeverry, C., Abin-Carriquiry, J.A., Blasina, F., Antúnez, K., Jones, D.P., Go, Y., Liang, Y., Dajas, F., 2010. After cellular internalization, quercetin causes Nrf2 nuclear translocation , increases glutathione levels , and prevents neuronal death against an oxidative insult. Free Radic. Biol. Med. 49, 738–747. https://doi.org/10.1016/j.freeradbiomed.2010.05.020.
Azuma, K., Ippoushi, K., Ito, H., Higashio, H., Terao, J., 2002. Combination of lipids and emulsifiers enhances the absorption of orally administered quercetin in rats. J. Agric. Food Chem. 50, 1706–1712. https://doi.org/10.1021/jf0112421.
Bennecib, M., Gong, C.X., Grundke-Iqbal, I., Iqbal, K., 2000. Role of protein phosphatase-2A and -1 in the regulation of GSK-3, cdk 5 and cdc 2 and the phosphorylation of tau in rat forebrain. FEBS Lett. 485, 87–93. https://doi.org/10.1016/S0014-5793(00)02203-1.
Bjelke, B., Andersson, K., Ogren, S.O., Bolme, P., 1991. Asphytic lesion: proliferation of tyrosine-hydroxylase-immunoreactive nerve cell bodies in the rat substantia nigra and functional changes in dopamine neurotransmission. Brain Res. 543, 1–9.
Blasina, F., Vaamonde, L., Silvera, F., Tedesco, A.C., Dajas, F., 2015. Intravenous nanosomes of quercetin improve brain function and hemodynamic instability after severe hypoxia in newborn piglets. Neurochem. Int. 89, 149–156. https://doi.org/10.1016/j.neuint.2015.08.007.
Chiral, M., Grongnet, J.-F., Plumier, J.-C., David, J.C., 2004. Effects of hypoxia on stress proteins in the piglet brain at birth. Pediatr. Res. 56, 775–782. https://doi.org/10.1203/01.PDR.0000142732.09325.61.
Dai, Y., Li, W., Zhong, M., Chen, J., Liu, Y., Cheng, Q., Li, T., 2014. Preconditioning and post-treatment with cobalt chloride in rat model of perinatal hypoxic-ischemic encephalopathy. Brain Dev. 36, 228–240. https://doi.org/10.1016/j.braindev.2013.04.007.
Dajas, F., 2012. Life or death: neuroprotective and anticancer effects of quercetin. J. Ethnopharmacol. 143, 383–396. https://doi.org/10.1016/j.jep.2012.07.005.
Dajas, F., Abin-Carriquiry, J.A.A., Arredondo, F., Blasina, F., Echeverry, C., Martínez, M., Rivera, F., Vaamonde, L.L., Martinez, M., Rivera, F., Vaamonde, L.L., Martínez, M., Rivera, F., Vaamonde, L.L., 2015. Quercetin in brain diseases: potential and limits. Neurochem. Int. 89, 140–148. https://doi.org/10.1016/j.neuint.2015.07.002.
Dajas, F., Rivera, F., Blasina, F., Arredondo, F., Echeverry, C., Lafon, L., Morquio, A., Heizen, H., 2003. Cell culture protection and in vivo neuroprotective capacity of flavonoids. Neurotox. Res. 5, 425–432. https://doi.org/10.1007/BF03033172.
Danaei, M., Dehghankhold, M., Ataei, S., Hasanzadeh Davarani, F., Javanmard, R., Dokhani, A., Khorasani, S., Mozafari, M.R., 2018. Impact of particle size and polydispersity index on the clinical applications of lipidic nanocarrier systems. Pharmaceutics. https://doi.org/10.3390/pharmaceutics10020057.
Davidson, J.O., Wassink, G., Heuij, L.G. Van Den, Bennet, L., Gunn, A.J., 2015. Therapeutic hypothermia for neonatal hypoxic – ischemic encephalopathy – where to from here? Front. Neurol. 6, 198. https://doi.org/10.3389/fneur.2015.00198.
Díaz, M., Vaamonde, L., Dajas, F., 2015. Assessment of the protective capacity of nanosomes of quercetin in an experimental model of Parkinson's disease in the rat. Gen. Med. Open Access 3, 1–7. https://doi.org/10.4172/2327-5146.1000207.
Dong, F., Wang, S., Wang, Y., Yang, X., Jiang, J., Wu, D., Qu, X., Fan, H., Yao, R., 2017. Quercetin ameliorates learning and memory via the Nrf2-ARE signaling pathway in D-galactose-induced neurotoxicity in mice. Biochem. Biophys. Res. Commun. 491, 636–641. https://doi.org/10.1016/j.bbrc.2017.07.151.
Du Plessis, A.J., Volpe, J.J., 2002. Perinatal brain injury in the preterm and term newborn. Curr. Opin. Neurol. 15, 151–157. https://doi.org/10.1097/00019052-200204000-00005.
Fleiss, B., Gressens, P., 2019. Neuroprotection of the preterm brain. In: Handbook of Clinical Neurology. Elsevier B.V., pp. 315–328. https://doi.org/10.1016/B978-0-444-64029-1.00015-1
Fukuda, T., Naiki, T., Saito, M., Irie, K., 2009. hnRNP K interacts with RNA binding motif protein 42 and functions in the maintenance of cellular ATP level during stress conditions. Gene Cell. 14, 113–128. https://doi.org/10.1111/j.1365-2443.2008.01256.x.
Ghosh, A., Sarkar, S., Mandal, A.K., Das, N., 2013. Neuroprotective role of nanoencapsulated quercetin in combating ischemia-reperfusion induced neuronal damage in young and aged rats. PloS One 8 (4), e57735. https://doi.org/10.1371/journal.pone.0057735.
Glass, H.C., 2018. Hypoxic-ischemic encephalopathy and other neonatal encephalopathies. Contin. Lifelong Learn. Neurol. 24, 57–71. https://doi.org/10.1212/CON.0000000000000557.
Gluckman, P.D., Wyatt, J.S., Azzopardi, D., Ballard, R., Edwards, A.D., Ferriero, D.M., Polin, R.A., Robertson, C.M., Thoresen, M., Whitelaw, A., Gunn, A.J., 2005. Selective head cooling with mild systemic hypothermia after neonatal encephalopathy: multicentre randomised trial. Lancet 365, 663–670. https://doi.org/10.1016/S0140-6736(05)17946-X.
Haque, A., Polcyn, R., Matzelle, D., Banik, N.L., 2018. New insights into the role of neuron-specific enolase in neuro-inflammation, neurodegeneration, and neuroprotection. Brain Sci. 8 (33) https://doi.org/10.3390/brainsci8020033.
Herrera-Marschitz, M., Morales, P., Leyton, L., Bustamante, D., Klawitter, V., Espina-Marchant, P., Allende, C., Lisboa, F., Cunich, G., Jara-Cavieres, A., Neira, T., Gutierrez-Hernandez, M.A., Gonzalez-Lira, V., Simola, N., Schmitt, A., Morelli, M., Tasker, R.A., Gebicke-Haerter, P.J., 2011. Perinatal asphyxia: current status and approaches towards neuroprotective strategies, with focus on sentinel proteins. Neurotox. Res. 19, 603–627. https://doi.org/10.1007/s12640-010-9208-9.
Hochachka, P.W., Lutz, P.L., 2001. Mechanism, origin, and evolution of anoxia tolerance in animals. In: Comparative Biochemistry and Physiology - B Biochemistry and Molecular Biology. Elsevier Inc, pp. 435–459. https://doi.org/10.1016/S1096-4959(01)00408-0.
Iwata, O., Iwata, S., Bainbridge, A., De Vita, E., Matsuishi, T., Cady, E.B., Robertson, N.J., 2008. Supra- and sub-baseline phosphocreatine recovery in developing brain after transient hypoxia-ischaemia: relation to baseline energetics, insult severity and outcome. Brain 131, 2220–2226. https://doi.org/10.1093/brain/awn150.
Kadota, S., Nagata, K., 2011. pp32, an INHAT component, is a transcription machinery recruiter for maximal induction of IFN-stimulated genes. J. Cell Sci. 124, 892–899. https://doi.org/10.1242/jcs.078253.
Keller, T., Körber, F., Oberthuer, A., Schafmeyer, L., Mehler, K., Kuhr, K., Kribs, A., 2019. Intranasal breast milk for premature infants with severe intraventricular hemorrhage—an observation. Eur. J. Pediatr. 178, 199–206. https://doi.org/10.1007/s00431-018-3279-7.
Kirova, Y.I., Germanova, E.L., Lukyanova, L.D., 2013. Phenotypic features of the dynamics of HIF-1α levels in rat neocortex in different hypoxia regimens. Bull. Exp. Biol. Med. 154 (6), 718–722. https://doi.org/10.1007/s10517-013-2038-z.
Kletkiewicz, H., Hyjek, M., Jaworski, K., Nowakowska, A., Rogalska, J., 2018. Activation of hypoxia-inducible factor-1α in rat brain after perinatal anoxia: role of body temperature. Int. J. Hyperther. 34, 824–833. https://doi.org/10.1080/02656736.2017.1385860.
Ko, C.C., Chen, Y.J., Chen, C.T., Liu, Y.C., Cheng, F.C., Hsu, K.C., Chow, L.P., 2014. Chemical proteomics identifies heterogeneous nuclear ribonucleoprotein (hnRNP) A1 as the molecular target of quercetin in its anti-cancer effects in PC-3 cells. J. Biol. Chem. 289, 22078–22089. https://doi.org/10.1074/jbc.M114.553248.
Kruse, T., Gnosa, S.P., Nasa, I., Garvanska, D.H., Hein, J.B., Nguyen, H., Samsøe-Petersen, J., Lopez-Mendez, B., Hertz, E.P.T., Schwarz, J., Pena, H.S., Nikodemus, D., Kveiborg, M., Kettenbach, A.N., Nilsson, J., 2020. Mechanisms of site-specific dephosphorylation and kinase opposition imposed by PP2A regulatory subunits. EMBO J. 39 https://doi.org/10.15252/embj.2019103695.
Kular, R.K., Cvetanovic, M., Siferd, S., Kini, A.R., Opal, P., 2009. Neuronal differentiation is regulated by leucine-rich acidic nuclear protein (LANP), a member of the inhibitor of histone acetyltransferase complex. J. Biol. Chem. 284, 7783–7792. https://doi.org/10.1074/jbc.M806150200.
Kumar, H., Mishra, G., Sharma, A.K., Gothwal, A., Kesharwani, P., Gupta, U., 2017. Intranasal drug delivery: a non-invasive approach for the better delivery of neurotherapeutics. Pharm. Nanotechnol. 5 (3) https://doi.org/10.2174/2211738505666170515113936.
Kurinczuk, J.J., White-Koning, M., Badawi, N., 2010. Epidemiology of neonatal encephalopathy and hypoxic-ischaemic encephalopathy. Early Hum. Dev. 86, 329–338. https://doi.org/10.1016/j.earlhumdev.2010.05.010.
Laptook, A.R., 2016. Birth asphyxia and hypoxic-ischemic brain injury in the preterm infant. Clin. Perinatol. 43, 529–545. https://doi.org/10.1016/j.clp.2016.04.010.
Le, K., Song, Z., Deng, J., et al., 2020. Quercetin alleviates neonatal hypoxic-ischemic brain injury by inhibiting microglia-derived oxidative stress and TLR4-mediated inflammation. Inflamm. Res. 69, 1201–1213. https://doi.org/10.1007/s00011-020-01402-5.
Lee, K., Roth, R.A., Lapres, J.J., 2007. Hypoxia, drug therapy and toxicity. Pharmacol. Ther. 113, 229–246. https://doi.org/10.1016/j.pharmthera.2006.08.001.
Lei, X., Chao, H., Zhang, Z., Lv, J., Li, S., Wei, H., Xue, R., Li, F., Li, Z., 2015. Neuroprotective effects of quercetin in a mouse model of brain ischemic/reperfusion injury via anti-apoptotic mechanisms based on the Akt pathway. Mol. Med. Rep. 12, 3688–3696. https://doi.org/10.3892/mmr.2015.3857.
Li, D., Song, T., Yang, L., Wang, X., Yang, C., Jiang, Y., 2016. Neuroprotective actions of pterostilbene on hypoxic-ischemic brain damage in neonatal rats through upregulation of heme oxygenase-1. Int. J. Dev. Neurosci. 54, 22–31. https://doi.org/10.1016/j.ijdevneu.2016.08.005.
Liu, L., Oza, S., Hogan, D., Chu, Y., Perin, J., Zhu, J., Lawn, J.E., Cousens, S., Mathers, C., Black, R.E., 2016. Global, regional, and national causes of under-5 mortality in 2000–15: an updated systematic analysis with implications for the Sustainable Development Goals. Lancet 388, 3027–3035. https://doi.org/10.1016/S0140-6736(16)31593-8.
Liu, R., Pei, J.J., Wang, X.C., Zhou, X.W., Tian, Q., Winbladt, B., Wang, J.Z., 2005. Acute anoxia induces tau dephosphorylation in rat brain slices and its possible underlying mechanisms. J. Neurochem. 94, 1225–1234. https://doi.org/10.1111/j.1471-4159.2005.03270.x.
Liu, Y., Szaro, B.G., 2011. HnRNP K post-transcriptionally co-regulates multiple cytoskeletal genes needed for axonogenesis. Development 138, 3079–3090. https://doi.org/10.1242/dev.066993.
Llanos, S., Efeyan, A., Monsech, J., Dominguez, O., Serrano, M., 2006. A high-throughput loss-of-function screening identifies novel p53 regulators. Cell Cycle 5, 1880–1885. https://doi.org/10.4161/cc.5.16.3140.
Mallard, C., Vexler, Z.S., 2015. Modeling ischemia in the immature brain: how translational are animal models? Stroke 46, 3006–3011. https://doi.org/10.1161/STROKEAHA.115.007776.
Mandel, S.A., Weinreb, O., Amit, T., Youdim, M.B.H., 2012. Molecular mechanisms of the neuroprotective/neurorescue action of multi-target green tea polyphenols. Front. Biosci. - Sch. 4 S 581–598. https://doi.org/10.2741/s286.
Martínez-Busi, M., Arredondo, F., González, D., Echeverry, C., Vega-Teijido, M.A., Carvalho, D., Rodríguez-Haralambides, A., Rivera, F., Dajas, F., Abin-Carriquiry, J. A., 2019. Purification, structural elucidation, antioxidant capacity and neuroprotective potential of the main polyphenolic compounds contained in

Achyrocline satureioides (Lam) D.C. (Compositae). Bioorg. Med. Chem. 27, 2579–2591. https://doi.org/10.1016/j.bmc.2019.03.047.
Marx, D., Williams, G., Birkhoff, M., 2015. Intranasal drug administration — an attractive delivery route for some drugs. In: Drug Discovery and Development - from Molecules to Medicine. In Drug Discovery and Development - from Molecules to Medicine. https://doi.org/10.5772/59468.
McAdams, R.M., Juul, S.E., 2016. Neonatal encephalopathy: update on therapeutic hypothermia and other novel therapeutics. Clin. Perinatol. 43 (3), 485–500. https://doi.org/10.1016/j.clp.2016.04.007.
Merchant, N., Azzopardi, D., 2015. Hipotermia y EHI - predictores precoces de Resultados. Dev. Med. Child Neurol. 57, 8–16. https://doi.org/10.1111/dmcn.12726.
Nitti, M., Piras, S., Brondolo, L., Marinari, U., Pronzato, M., Furfaro, A., 2018. Heme oxygenase 1 in the nervous system: does it favor neuronal cell survival or induce neurodegeneration? Int. J. Mol. Sci. 19, 2260. https://doi.org/10.3390/ijms19082260.
Odd, D.E., Lewis, G., Whitelaw, A., Gunnell, D., 2009. Resuscitation at birth and cognition at 8 years of age: a cohort study. Lancet 373, 1615–1622. https://doi.org/10.1016/S0140-6736(09)60244-0.
Onténiente, B., Rasika, S., Benchoua, A., Guégan, C., 2003. Molecular pathways in cerebral ischemia necrosis vs Apoptosis : the quest. Mol. Neurobiol. 27, 33–72.
Osier, N., McGreevy, E., Pham, L., Puccio, A., Ren, D., Conley, Y.P., Alexander, S., Dixon, C.E., 2018. Melatonin as a therapy for traumatic brain injury: a review of published evidence. Int. J. Mol. Sci. 19 (5), 1539. https://doi.org/10.3390/ijms19051539.
Ossola, B., Kääriäinen, T.M., Männistö, P.T., 2009. The multiple faces of quercetin in neuroprotection. Expet Opin. Drug Saf. 8 (4), 397–409. https://doi.org/10.1517/14740330903026944.
Patil, C.S., Singh, V.P., Satyanarayan, P.S.V., Jain, N.K., Singh, A., Kulkarni, S.K., 2003. Protective effect of flavonoids against aging- and lipopolysaccharide-induced cognitive impairment in mice. Pharmacology 69, 59–67. https://doi.org/10.1159/000072357.
Pfaffl, M.W., Horgan, G.W., Dempfle, L., 2002. Relative expression software tool (REST) for group-wise comparison and statistical analysis of relative expression results in real-time PCR. Nucleic Acids Res. 30, e36. https://doi.org/10.1093/nar/30.9.e36.
Pierson, C.R., Folkerth, R.D., Billiards, S.S., Trachtenberg, F.L., Drinkwater, M.E., Volpe, J.J., Kinney, H.C., 2007. Gray matter injury associated with periventricular leukomalacia in the premature infant. Acta Neuropathol. 114, 619–631. https://doi.org/10.1007/s00401-007-0295-5.
Poitz, D.M., Augstein, A., Hesse, K., et al., 2014. Regulation of the HIF-system in human macrophages – differential regulation of HIF-α subunits under sustained hypoxia. Mol. Immunol. 57, 226–235. https://doi.org/10.1016/j.molimm.2013.10.001, 2014.
Qu, X., Qi, D., Dong, F., Wang, B., Guo, R., Luo, M., Yao, R., 2014. Quercetin improves hypoxia-ischemia induced cognitive deficits via promoting remyelination in neonatal rat. Brain Res. 17 (1553), 31–40. https://doi.org/10.1016/j.brainres.2014.01.035.
Rainaldi, M.A., Perlman, J.M., 2016. Pathophysiology of birth asphyxia. Clin. Perinatol. 43, 409–422. https://doi.org/10.1016/j.clp.2016.04.002.
Rao, R., Trivedi, S., Vesoulis, Z., Liao, S., Smyser, C., Mathur, A., 2017. Safety and short term outcomes of therapeutic hypothermia in preterm neonates 34-35 weeks gestational age with Hypoxic Ischemic Encephalopathy. J. Pediatr. 183, 37–42.
Rendeiro, C., Spencer, J.P.E., Vauzour, D., Butler, L.T., Ellis, J.A., Williams, C.M., 2009. The impact of flavonoids on spatial memory in rodents: from behaviour to underlying hippocampal mechanisms. Genes Nutr 4, 251–270. https://doi.org/10.1007/s12263-009-0137-2.
Rivera, F., Costa, G., Abin, A., Urbanavicius, J., Arruti, C., Casanova, G., Dajas, F., 2008. Reduction of ischemic brain damage and increase of glutathione by a liposomal preparation of quercetin in permanent focal ischemia in rats. Neurotox. Res. 13, 105–114. https://doi.org/10.1007/BF03033562.
Rivera, F., Urbanavicius, J., Gervaz, E., Morquio, A., Dajas, F., Riveraa, F., Urbanaviciusa, J., Gervazb, E., Morquioa, A., Dajasa, F., Rivera, F., Urbanavicius, J., Gervaz, E., Morquio, A., Dajas, F., Riveraa, F., Urbanaviciusa, J., Gervazb, E., Morquioa, A., Dajasa, F., 2004. Some aspects of the in vivo neuroprotective capacity of flavonoids: bioavailability and structure-activity relationship. Neurotox. Res. 6, 543–553. https://doi.org/10.1007/BF03033450.
Rodríguez, M., Valez, V., Cimarra, C., Blasina, F., Radi, R., 2020. Hypoxic-ischemic encephalopathy and mitochondrial dysfunction: facts, unknowns, and challenges. Antioxidants Redox Signal. 33 (4), 1–44. https://doi.org/10.1089/ars.2020.8093.
Roth, J.A., Tuggle, C.K., 2015. Livestock models in translational medicine. ILAR J. 56 (1), 1–6. https://doi.org/10.1093/ilar/ilv011.
Schindelin, J., Arganda-Carreras, I., Frise, E., Kaynig, V., Longair, M., Pietzsch, T., Preibisch, S., Rueden, C., Saalfeld, S., Schmid, B., Tinevez, J.-Y., White, D.J., Hartenstein, V., Eliceiri, K., Tomancak, P., Cardona, A., 2012. Fiji: an open-source platform for biological-image analysis. Nat. Methods 9, 676–682. https://doi.org/10.1038/nmeth.2019.
Semenza, G.L., 2004. Hydroxylation of HIF-1: oxygen sensing at the molecular level. Physiology 19, 176–182. https://doi.org/10.1152/physiol.00001.2004.
Semenza, G.L., Jiang, B.H., Leung, S.W., Passantino, R., Concordat, J.P., Maire, P., Giallongo, A., 1996. Hypoxia response elements in the aldolase A, enolase 1, and lactate dehydrogenase a gene promoters contain essential binding sites for hypoxia-inducible factor 1. J. Biol. Chem. 271, 32529–32537. https://doi.org/10.1074/jbc.271.51.32529.
Shah, F.-A., Park, D.-J., Gim, S.-A., Koh, P.-O., 2015. Curcumin treatment recovery the decrease of protein phosphatase 2A subunit B induced by focal cerebral ischemia in Sprague-Dawley rats. Lab. Anim. Res. 31, 134. https://doi.org/10.5625/lar.2015.31.3.134.
Shah, F.A., Park, D.J., Koh, P.-O., 2018. Identification of proteins differentially expressed in the striatum by melatonin in a middle cerebral artery occlusion rat model—a proteomic and in silico approach. Neurochem. Res. 43, 1608–1623. https://doi.org/10.1007/s11064-018-2576-x.
Shankaran, S., 2012. Hypoxic-ischemic encephalopathy and novel strategies for neuroprotection. Clin. Perinatol. 39 (4), 919–929. https://doi.org/10.1016/j.clp.2012.09.008.
Sharma, D.R., Wani, W.Y., Sunkaria, A., Kandimalla, R.J., Sharma, R.K., Verma, D., Bal, A., Gill, K.D., 2016. Quercetin attenuates neuronal death against aluminum-induced neurodegeneration in the rat hippocampus. Neuroscience 324, 163–176. https://doi.org/10.1016/j.neuroscience.2016.02.055.
Shi, Y., 2009. Serine/threonine phosphatases: mechanism through structure. Cell 139 (3), 468–484. https://doi.org/10.1016/j.cell.2009.10.006.
Shih, A.Y., Imbeault, S., Barakauskas, V., Erb, H., Jiang, L., Li, P., Murphy, T.H., 2005. Induction of the Nrf2-driven antioxidant response confers neuroprotection during mitochondrial stress in vivo. J. Biol. Chem. 280, 22925–22936. https://doi.org/10.1074/jbc.M414635200.
Shoshan-Barmatz, V., Krelin, Y., Shteinfer-Kuzmine, A., 2018. VDAC1 functions in Ca2+ homeostasis and cell life and death in health and disease. Cell Calcium 69, 81–100. https://doi.org/10.1016/j.ceca.2017.06.007.
Silva, J.P., Gomes, A.C., Coutinho, O.P., 2008. Oxidative DNA damage protection and repair by polyphenolic compounds in PC12 cells. Eur. J. Pharmacol. 601, 50–60. https://doi.org/10.1016/j.ejphar.2008.10.046.
Srivastava, S., Somasagara, R.R., Hegde, M., Nishana, M., Tadi, S.K., Srivastava, M., Choudhary, B., Raghavan, S.C., 2016. Quercetin, a natural flavonoid interacts with DNA, arrests cell cycle and causes tumor regression by activating mitochondrial pathway of apoptosis. Sci. Rep. 6, 24049. https://doi.org/10.1038/srep24049.
Suzuki, Y., Nakagomi, S., Namikawa, K., Kiryu-Seo, S., Inagaki, N., Kaibuchi, K., Aizawa, H., Kikuchi, K., Kiyama, H., 2003. Collapsin response mediator protein-2 accelerates axon regeneration of nerve-injured motor neurons of rat. J. Neurochem. 86, 1042–1050. https://doi.org/10.1046/j.1471-4159.2003.01920.x.
Szklarczyk, D., Gable, A., Lyon, D., Junge, A., Wyder, S., Huerta-cepas, J., Simonovic, M., Doncheva, N., Morris, J., Bork, P., Jensen, L., von Mering, C., 2019. STRING v11: protein-protein association networks with increased coverage, supporting functional discovery in genome-wide experimental datasets. Nucleic Acids Res. 47, D607–D613.
Thoresen, M., Penrice, J., Lorek, A., Cady, E.B., Wylezinska, M., Kirkbride, V., Cooper, C. E., Brown, G.C., Edwards, A.D., Wyatt, J.S., Reynolds, E.O., 1995. Mild hypothermia after severe transient hypoxia-ischemia ameliorates delayed cerebral energy failure in the newborn piglet. Pediatr. Res. 37, 667–670. https://doi.org/10.1203/00006450-199505000-00019.
Triantafyllou, A., Liakos, P., Tsakalof, A., Chachami, G., Paraskeva, E., Molyvdas, P.-A., Georgatsou, E., Simos, G., Bonanou, S., 2007. The flavonoid quercetin induces hypoxia-inducible factor-1 alpha (HIF-1α) and inhibits cell proliferation by depleting intracellular iron. Free Radic. Res. 41, 342–356. https://doi.org/10.1080/10715760601055324.
van Bel, F.V., Groenendaal, F., 2016. Drugs for neuroprotection after birth asphyxia: pharmacologic adjuncts to hypothermia. Semin. Perinatol. 40, 152–159. https://doi.org/10.1053/j.semperi.2015.12.003.
Van Elzen, R., Moens, L., Dewilde, S., Elzen, R. Van, Moens, L., Dewilde, S., 2008. Expression profiling of the cerebral ischemic and hypoxic response. Expert Rev. Proteomics 5, 263–282. https://doi.org/10.1586/14789450.5.2.263.
Van Erp, T.G.M., Saleh, P.A., Rosso, I.M., Huttunen, M., Lönnqvist, J., Pirkola, T., Salonen, O., Valanne, L., Poutanen, V.P., Standertskjöld-Nordenstam, C.G., Cannon, T.D., 2002. Contributions of genetic risk and fetal hypoxia to hippocampal volume in patients with schizophrenia or schizoaffective disorder, their unaffected siblings, and healthy unrelated volunteers. Am. J. Psychiatr. 159, 1514–1520. https://doi.org/10.1176/appi.ajp.159.9.1514.
Vannucci, S.J., Hagberg, H., 2004. Hypoxia-ischemia in the immature brain. J. Exp. Biol. 207, 3149–3154. https://doi.org/10.1242/jeb.01064.
Wang, S., Wang, Y., Lu, Q., Liu, X., Wang, F., Ma, X., Cui, C., Shi, C., Li, J., Zhang, D., 2015. The expression and distributions of ANP32A in the developing brain. BioMed Res. Int. https://doi.org/10.1155/2015/207347, 2015, ID 207347.
Weitzdörfer, R., Höger, H., Burda, G., Pollak, A., Lubec, G., Weitzdörfer, R., Höger, H., Burda, G., Pollak, A., Lubec, G., 2008. Differences in hippocampal protein expression at 3 days, 3 weeks, and 3 months following induction of perinatal asphyxia in the rat. J. Proteome Res. 7, 1945–1952. https://doi.org/10.1021/pr700835y.
Wenger, R.H., Kvietikova, I., Rolfs, A., Gassmann, M., Marti, H.H., 1997. Hypoxia-inducible factor-1α is regulated at the post-mRNA level. In: Kidney International. Nature Publishing Group, pp. 560–563. https://doi.org/10.1038/ki.1997.79.
Yang, M., Chowdhury, R., Ge, W., Hamed, R.B., McDonough, M.A., Claridge, T.D.W., Kessler, B.M., Cockman, M.E., Ratcliffe, P.J., Schofield, C.J., 2011. Factor-inhibiting hypoxia-inducible factor (FIH) catalyses the post-translational hydroxylation of histidinyl residues within ankyrin repeat domains. FEBS J. 278, 1086–1097. https://doi.org/10.1111/j.1742-4658.2011.08022.x.
Zhang, Q., Pi, J., Woods, C.G., Andersen, M.E., 2010. A systems biology perspective on Nrf2-mediated antioxidant response. Toxicol. Appl. Pharmacol. 244 (1), 84–97. https://doi.org/10.1016/j.taap.2009.08.018.
Zhu, M., Ding, J., Jiang, H., Kong, L., Sun, Z., Chen, J., Miao, C., 2015. Propofol ameliorates endothelial inflammation induced by hypoxia/reoxygenation in human umbilical vein endothelial cells: role of phosphatase A2. Vasc. Pharmacol. 73, 149–157. https://doi.org/10.1016/j.vph.2015.06.002.